Journal of Medicinal Chemistry

ARTICLE

pubs.acs.org/jmc

Optimization of Potent, Selective, and Orally Bioavailable Pyrrolodinopyrimidine-Containing Inhibitors of Heat Shock Protein 90. Identification of Development Candidate 2-Amino-4-{4-chloro-2-[2-(4-fluoro-1*H*-pyrazol-1-yl)ethoxy]-6-methylphenyl}-*N*-(2,2-difluoropropyl)-5,7-dihydro-6*H*-pyrrolo[3,4-*d*]pyrimidine-6-carboxamide

Luke Zehnder, Michael Bennett, Jerry Meng, Buwen Huang, Sacha Ninkovic, Fen Wang, John Braganza, John Tatlock, Tanya Jewell, Joe Zhongxiang Zhou, Ben Burke, Jeff Wang, Karen Maegley, Pramod P. Mehta, Min-Jean Yin, Ketan S. Gajiwala, Michael J. Hickey, Shinji Yamazaki, Evan Smith, Ping Kang, Anand Sistla, Elena Dovalsantos, Michael R. Gehring, Robert Kania, Martin Wythes, and Pei-Pei Kung*

La Jolla Laboratories, Pfizer Worldwide Research and Development, 10770 Science Center Drive, San Diego, California 92121, United States

Supporting Information

ABSTRACT: A novel class of heat shock protein 90 (Hsp90) inhibitors was discovered by high-throughput screening and was subsequently optimized using a combination of structure-based design, parallel synthesis, and the application of medicinal chemistry principles. Through this process, the biochemical and cell-based potency of the original HTS lead were substantially improved along with the corresponding metabolic stability properties. These efforts culminated with the identification of a development candidate (compound **42**) which displayed desired PK/PD relationships, significant efficacy in a melanoma A2058 xenograft tumor model, and attractive DMPK profiles.

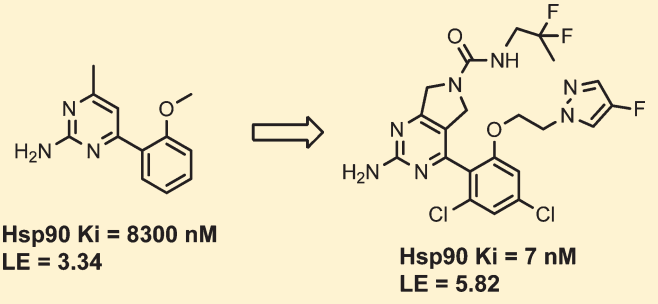

INTRODUCTION

Molecular chaperones are attractive targets for cancer therapy because of their roles in regulating many proteins involved in signaling pathways and cell proliferation. One such molecular chaperone, heat shock protein 90 (Hsp90), was identified in 1987 as one of the most abundant intracellular proteins.[1] Hsp90 functions to promote the maturation and conformational stabilization of its client proteins which include many kinases (Her2, Akt, Raf, and Cdk 4), receptors (androgen and estrogen receptors), and transcription factors (Hif1α).[2] As many of these client proteins have been implicated as key regulators of oncogenic signaling and/or cell proliferation,[3] inhibition of Hsp90 chaperone activity represents a novel approach for the identification of new cancer therapies.

Hsp90 is an ATPase and undergoes large conformational changes during the course of its ATP cycle and upon binding certain Hsp90 cochaperones.[4] The N-terminal domain of the protein contains an adenine triphosphate (ATP) binding site, and most of the Hsp90 inhibitors identified to date associate with this ATP binding pocket. The shape of the Hsp90 ATP binding pocket is unique[5] compared to other ATPase and kinases, and the isolated ATP-binding domain has low intrinsic ATPase activity.[6] The natural product geldanamycin (GA, **1a**, Figure 1) was first identified as an Hsp90 inhibitor in 1994.[7] Its semisynthetic analogues 17-allylamino-17-demethoxygeldanamycin (17-AAG, **1b**, Figure 1) and 17-dimethylaminoethylamino-17-demethoxygeldanamycin (DMAG, **1c**, Figure 1) have been developed as less toxic analogues.[8] 17-AAG was the first Hsp90 inhibitor to enter clinical trials, and although antitumor activity was observed in early assessments of the compound, the poor solubility and limited oral bioavailability of this agent may limit its future utility.[9] A prodrug of 17-AAG (IPI-504) has been identified that improves the pharmaceutical features of 17-AAG and is currently reported to be in phase II/III clinical trials.[10]

In the past several years, significant progress has been made in identifying non-quinone-containing small molecule Hsp90 inhibitors (recently reviewed by Janin[11]), and several such compounds are currently undergoing clinical trials as intravenously or orally administered agents. The latter compounds, orally bioavailable molecules reported in the literature, include CNF2024,[12] SNX5422,[13] and NVP-BEP800[14] (**2**, **3**, **4**, respectively, Figure 2). In spite of these advances, there remains a need for the

Received: February 5, 2011
Published: March 25, 2011

identification of new small molecule Hsp90 inhibitors with improved potency, pharmacokinetic properties, and safety profiles relative to existing anti-Hsp90 agents. In this report, we describe our medicinal chemistry efforts that afforded a novel class of Hsp90 inhibitors that exhibit potent efficacy in animal tumor models along with other desirable pharmaceutical properties.

RESULT AND DISCUSSION

Our Hsp90 research program began with a high throughput screening campaign using a competition binding assay in which the ability of test compounds to displace a tritium-labeled resorcinol amide related to compound **5** (Supporting Information) from Hsp90 was assessed. This effort led to the discovery of the 4-methyl-2-aminopyrimidine-containing inhibitor **6** (Table 1) which displayed a K_i of 1.2 μM in the binding assay and an IC_{50} of greater than 50 μM in a cell-based assay which examined the degradation of the Hsp90 client protein Akt.[3] The calculated ligand efficiency[15] (LE = 0.53) and ligand lipophilicity efficiency[16] (LipE = 4.25) for **6** using its K_i were both considered acceptable for initiating further structure−activity optimization efforts. However, we were concerned that the chlorine atom contained in **6** might be biologically reactive and/or unstable,[17] and we therefore replaced this substituent with a methyl group. Although the resulting compound (**7**, Table 1, LipE = 3.34) displayed somewhat reduced Hsp90 inhibitory activity and LipE relative to **6**, it was considered to be a better starting point for SAR development and property optimization because of its lack of obvious structural liabilities.

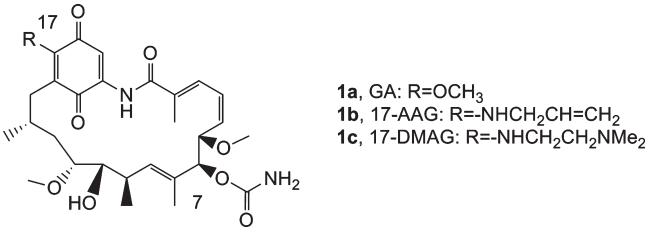

Figure 1. Geldanamycin and its semisynthetic derivatives.

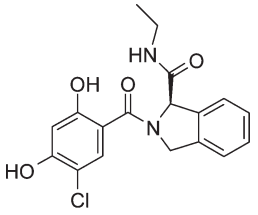

5

To facilitate potency improvements we obtained a 1.7 Å cocrystal structure of compound **6** bound to Hsp90 (Figure 3, PDB code 3R4M) and compared it to the corresponding cocrystal structure of a potent resorcinol amide Hsp90 inhibitor (compound **5**, K_i = 13 nM).[18,19] This analysis (Figure 3) suggested that addition of an *o*-chlorine atom to the phenyl ring of **6** or **7** (vide infra) would duplicate key space-filling interactions with the Hsp90 protein made by the chlorine present in

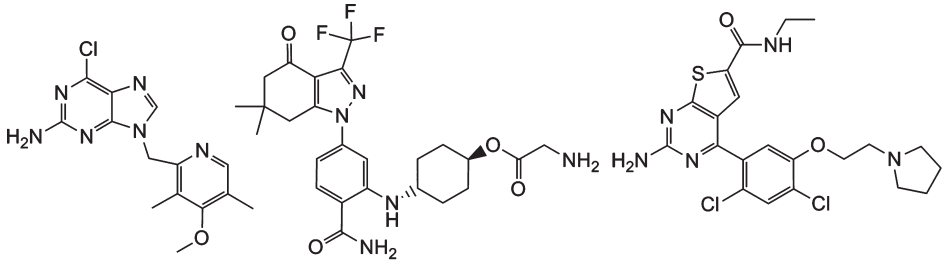

Figure 2. Structures of known orally bioavailable Hsp90 non-benzoquinone inhibitors.

Table 1. SAR around the Phenyl Moiety of Compound 7

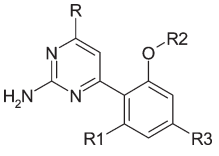

Compound#	R	R1	R2	R3	Enzyme K_i[a] (μM)	Cell IC_{50}[b] (μM)
6	Cl	H	CH_3	H	1.2	>50
7	CH_3	H	CH_3	H	8.3	ND
8	CH_3	Cl	CH_3	H	0.7	>10
9	CH_3	Cl	H	H	1.4	ND
10	CH_3	Cl	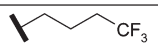	H	0.13	7.3
11	CH_3	Cl	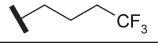	Cl	0.05	1.9

[a] Enzymatic K_i was calculated from enzymatic IC_{50} using the Cheng−Prusoff equation. Assay error is 10−15%. [b] Assay error is 10−15%.

dx.doi.org/10.1021/jm200128m |*J. Med. Chem.* 2011, 54, 3368–3385

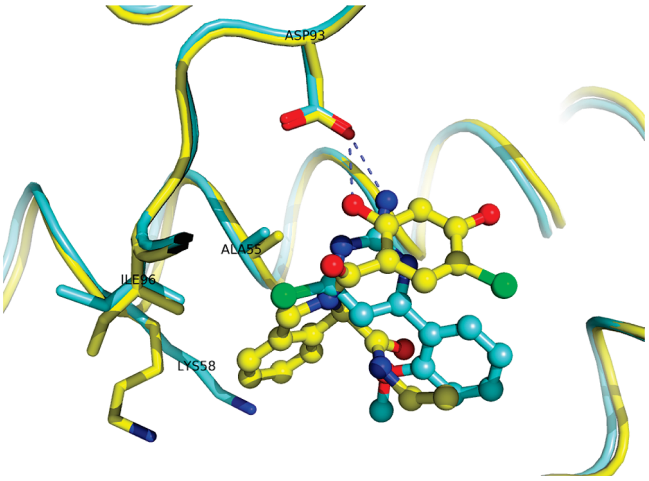

Figure 3. Overlap of bound conformations of **6** and **5**.

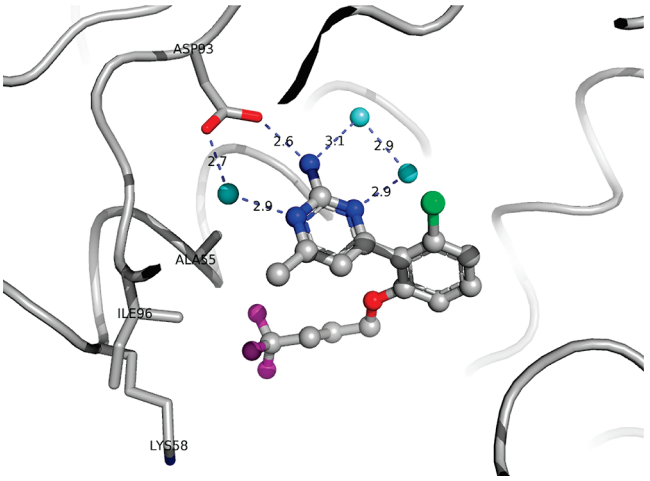

Figure 4. Crystal structure of **10** bound to the Hsp90 enzyme.

resorcinol **5**. Encouragingly, introduction of such an *o*-chloro moiety into the 2-aminopyrimidine scaffold afforded a molecule that displayed 10-fold improved Hsp90 inhibition relative to the unsubstituted compound (compare **8** with **7**; Table 1). However, the new inhibitor **8** did not exhibit measurable activity in the cell-based assay, indicating the need for further potency and/or property improvements.

Examination of the cocrystal structure of **6** with Hsp90 protein suggested that the methoxy moiety present in **6** made beneficial space-filling interactions with the protein. Not surprisingly, replacement of the methoxy group present in inhibitor **8** with a phenol resulted in a slight loss of anti-Hsp90 activity in the biochemical assay (compound **9**, Table 1). Seeking to recover and improve Hsp90 inhibition activity, we rapidly explored diverse substitution of the phenolic oxygen present in **9** using parallel synthesis methods (~100 compounds prepared). One compound identified by this parallel synthesis effort (**10**) displayed significantly improved Hsp90 enzyme inhibitory potency relative to both phenol **9** and the methoxy-containing inhibitor **8** (Table 1). Importantly, compound **10** also exhibited measurable anti-Hsp90 activity in the cell-based assay (IC_{50} = 7.3 μM). Encouraged by this result, we focused our optimization efforts on further improving the biochemical and cell-based Hsp90 inhibition properties of compound **10**.

Accordingly, we obtained a 2.0 Å cocrystal structure of **10** bound to Hsp90 (Figure 4, PDB code 3R4N) and observed that the trifluorobutyl group occupied the same hydrophobic pocket (formed by Lys58, ILE96, and Ala55) that was filled by the isoindoline moiety of resorcinol amide **5** (cf. Figure 4). This cocrystal structure also revealed a vacant hydrophobic pocket surrounding the para-position of the phenyl moiety present in **10** and suggested that addition of a lipophilic substituent to this portion of the inhibitor might improve Hsp90 binding affinity. The dichloro-containing molecule **11** was therefore prepared, and it exhibited more potent anti-Hsp 90 activity relative to **10** in both the biochemical and cell-based assays (Table 1). This improvement, however, came at the expense of ligand lipophilicity efficiency relative to lead compound **7** (LipE = 3.13 vs 3.34). Unfortunately, compound **11** also displayed moderate activity in a high-throughput ligand displacement assay designed to assess its potential to block human ether-a-go-go-related gene (hERG) ion channel function (dofetilide displacement;[20] K_i = 11.6 μM). The ratio of hERG IC_{50} values relative to the compound's cell potency was calculated to better define the separation between desired anti-Hsp90 activity and unwanted off-target effects ("therapeutic index", TI). To increase the window between desired anti-Hsp90 cellular activity and the undesired hERG affinity from **6** (TI = 6), we focused our research efforts on further improving the inhibitory potency of the 2-aminopyrimidine-containing compounds.

Toward this end, we incorporated a pyrrolourea moiety into our inhibitor scaffold that was anticipated to form beneficial hydrogen bonds with the side chain of Asn106 and backbone amide carbonyl of Gly97 (Figure 5). Similar interactions with Gly97 have also been noted by others to be important for obtaining Hsp90 inhibitory potency,[21,25] and analysis/modeling performed with the Hsp90-**10** cocrystal structure suggested the pyrrolourea as a good moiety to form these desired protein−ligand contacts. The resulting compound (**12**, Table 2) exhibited somewhat improved biochemical and cell-based Hsp90 inhibition properties relative to **11** along with more attractive ligand lipophilicity efficiency (LipE = 4.47 vs 3.13). The additional hydrogen bonds anticipated to be formed between the new inhibitor scaffold and the Hsp90 protein were confirmed by subsequently obtaining a cocrystal structure of a related inhibitor (**16**, Figure 6; PDB code 3R4O). Importantly, the new design also provided a vector off the urea moiety that could be utilized to explore additional space-filling interactions with the enzyme in order to further improve potency.

Four additional compounds (**13**−**16**, Table 2) using commercially available amines were then synthesized to develop the SAR associated with varying the urea substituent present in **12**. This effort identified several molecules that exhibited biochemical Hsp90-binding activity similar to that displayed by **12** (inhibitors **12**−**16**, Table 2). Compound **1c** (Figure 1) was also evaluated in the same biochemical and cellular assays as a comparison (Table 2, entry 1). One of these compounds (**16**, LipE = 4.55) also exhibited significantly improved anti-Hsp90 cell-based activity relative to the other inhibitors, albeit at the expense of in vitro human liver microsomal (HLM) stability. Although the exact reason for the cell-based improvement was not known with certainty, we nevertheless focused our efforts on preparing additional cyclobutylurea-containing inhibitors with the goal of further improving both cell-based activity and microsomal stability.

Accordingly, we combined the cyclobutylurea moiety with multiple phenol substituents that varied in size, shape, and polarity (**17**−**26**, Table 3). Some of these combinations afforded

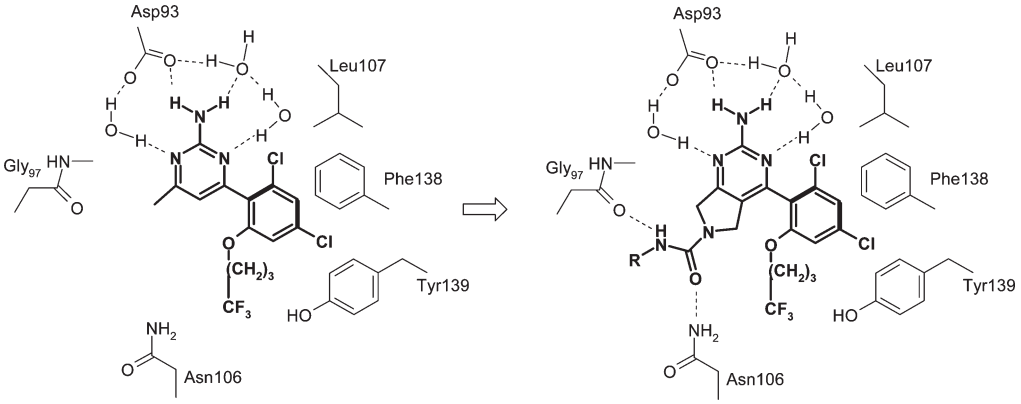

Figure 5. Design of pyrrolodinopyrimidine Hsp90 inhibitors.

Table 2

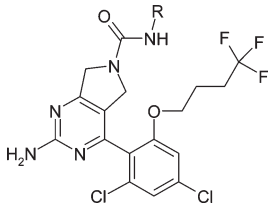

Compound#	R	Enzyme K_i[a] (μM)	Cell IC_{50}[b] (μM)	clogP	HLM CLint[c] (μL/min/mg)
1c	NA	0.68	0.1	2.4	12.3
12		0.026	0.95	3.1	56
13	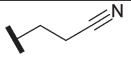	0.038	1.8	2.4	<8
14		0.021	0.84	3.3	<8
15		0.018	1.70	3.2	12.2
16		0.007	0.18	3.6	55.3

[a] Enzymatic K_i was calculated from enzymatic IC_{50} using the Cheng−Prusoff equation. Assay error is 10−15%. [b] Assay error is 10−15%. [c] CLint is intrinsic clearance.

inhibitors with comparable or improved microsomal stability relative to **16**, but only one (**26**) also exhibited similarly potent cell-based activity. Since the pyrazole-containing inhibitor **26** was considerably less lipophilic than **16** (clogP = 2.6 vs 3.6, respectively; LipE = 5.62 vs 4.55, respectively), we viewed the former molecule as an attractive starting point for continued optimization. Many additional pyrazole-containing compounds where then synthesized in which the urea substituent was again altered (Table 4). A multidimensional approach was employed to in vitro metabolic stability in which some of the new designs further lowered compound lipophilicity relative to **26** (**27**−**30**, Table 4) while others incorporated functional groups (e.g., F atoms) expected to block potential sites of oxidation of the cyclobutyl urea moiety in the molecules (**31** and **32**, Table 4). A few hybrid designs were also prepared that incorporated elements of both of these strategies (**33**−**35**, Table 4).

Encouragingly, many of these pyrazole-containing combinations exhibited significantly better stability in the in vitro microsomal assay relative to **26** and also displayed comparable or improved anti-Hsp90 cell-based activity (**30**−**35**, Table 4). These molecules also maintained the high ligand lipophilicity efficiency exhibited by other pyrazole-containing inhibitors (LipE = 5.62−6.09). To help differentiate these new molecules, we profiled them in assays designed to assess their in vitro permeability as well as their potential to form reactive metabolites upon metabolic activation. Incubation of compound **33** with human liver microsomes in the presence of glutathione (GSH) led to significant formation of GSH adducts (data not shown). This result suggested the significant formation of metabolism-derived reactive metabolites from **33**, and additional characterization of the compound was therefore deprioritized in favor of the other inhibitors (all of which exhibited this behavior to a much lower extent; data not shown). In addition, the low Caco-2

dx.doi.org/10.1021/jm200128m |*J. Med. Chem.* 2011, 54, 3368–3385

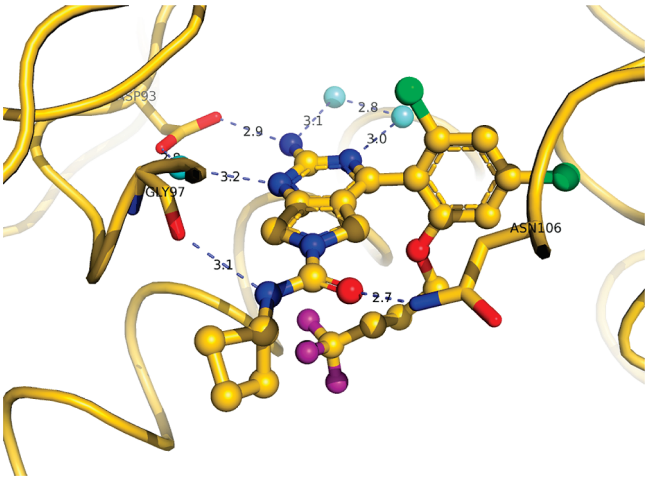

Figure 6. Crystal structure of **16** bound to the Hsp90 enzyme. The urea moiety of **16** forms additional hydrogen-bond interactions with Asn106 and Gly97 of Hsp90 protein.

apical to basolateral (AB)[22] value measured for inhibitor **30** (Table 4) suggested a poor potential to exhibit acceptable absorption following oral administration, and this molecule was similarly deprioritized.

The remaining inhibitors were profiled in assays designed to assess their ability to inhibit the cytochrome P450 3A4 (CYP3A4) enzyme as well as their potential to block hERG (IKr)[23] function. In each case, the ratio of CYP3A4 and hERG IC_{50} values relative to the compound's cell potency was calculated to better define the separation between desired anti-Hsp90 activity and unwanted off-target effects (TI). The binding of the compounds to human plasma proteins was also determined so that the impact of such association could be reflected in the in vitro metabolic stability assessments (i.e., determine unbound HLM clearance values). As shown in Table 5, the CYP3A4 inhibition noted for compounds **32**, **34**, and **35** exhibited was >10-fold weaker than the corresponding cell IC_{50} values. An even larger TI (>100) was noted when comparing the compounds' IKr and cell assay activities. To improve the potential for clinical success, we sought to increase the TI values for the series against both CYP3A4 and IKr by further improving cellular potency without compromising other desirable pharmaceutical properties.

To assist with this activity, the cocrystal structure of **35** in complex with the Hsp90 enzyme was obtained (Figure 7, PDB code 3R4P). Analysis of this cocrystal structure identified a small hydrophobic pocket surrounding the pyrazole moieties of the inhibitor. In an attempt to fill this pocket, a methyl or chloride atom was introduced at the C3-position of the pyrazole to increase hydrophobic interactions between the compounds and the Hsp90 enzyme. Unfortunately, the resulting 3-methylpyrazole (**36**) lost cellular potency relative to the unsubstituted inhibitor (**32**). In contrast, the 3-chloropyrazole-containing compound (**37**) displayed cellular potency equivalent to that of **32** but, likely due to a clogP increase of 0.8 units, also displayed increased HLM clearance. In an attempt to minimize increases in compound lipophilicity while simultaneously filling the small Hsp90 hydrophobic pocket, a fluorine atom was introduced at the 3-position of the pyrazole moiety present in compounds **32**, **34**, and **35**. Encouragingly, the resulting new molecules exhibited improved cellular potency relative to the original compounds (**38** with **32**, **39** with **34**, and **41** with **35**, Table 5). Unfortunately, inhibitor **38** exhibited higher metabolic clearance properties relative to **32** after correcting for protein binding effects.[24] In addition, compounds **39** and **41** displayed greater CYP3A4 and IKr inhibition relative to **34** and **35**, resulting in nearly identical TI values for the four compounds. We speculated that the higher lipophilicity of **39** and **41** was responsible for their increased CYP3A4 inhibition and subsequently explored reducing such lipophilicity by replacing the *o*-chloro atom in each molecule with a methyl group. The two 6-methylphenyl-containing compounds (**40** and **42**, Table 5) maintained good anti-Hsp90 cell-based activity, exhibited good in vitro stability toward human liver microsomes, and displayed increased CYP3A4 and IKr TI values relative to the 2-chlorophenyl-containing analogues. Among the compounds listed in Table 5, compound **42** (LipE = 5.82) exhibited the highest CYP3A4 and IKr TI values and was therefore selected for further in vitro and in vivo evaluation.

Compound **42** displayed attractive in vitro HLM CL, permeability, solubility (Table 6), minimal undesired hERG activity (IKr IC_{50}, Table 5), and a low potential to cause unwanted drug−drug interactions (DDI IC_{50}, Table 6). The compound was therefore assessed in both rat and dog in vivo pharmacokinetic studies where it displayed oral bioavailability of 15−20% in rats and 50−60% in dogs (Table 7). The oral bioavailability values in rats and dogs were consistent with their in vivo clearance value (77 and 8.4 mL/min/kg, respectively), suggesting near complete absorption (>90%) in both rats and dogs. Encouragingly, high volumes of distribution for **42** were noted in both rat and dog, and as a likely result, the compound exhibited a long half-life in both species. Similar oral bioavailability results were observed using amorphous and crystalline forms of the compound.

Compound **42** also displayed potent antiproliferation effects across a wide range of cell lines representing different human cancers. The IC_{50} values obtained by testing the compound against some of these lines are shown in Table 8. The ability of **42** to modulate pharmacodynamic biomarkers, such as Akt and Her2, in a melanoma cell line (A2058) was also determined in a single dose PK/PD experiment. Thus, compound **42** was dosed intraperitoneally (ip) in rats at 50 mg/kg and the plasma samples were subsequently taken after 4, 7, 24, 48, and 72 h. The compound maintained unbound plasma levels >2-fold above its in vitro IC_{50} (20 nM) for up to 7 h (Figure 8). In these experiments, the plasma levels of the Hsp90 client proteins (Akt and Her2) were observed to be lower (40−60%) than the control group for up to 72 h. The prolonged on-target effects of **42** on both Akt and Her2 protein levels could be due to the retention of compound in the target tumor,[25] although other explanations are possible. Encouraged by these results, we further evaluated the in vivo efficacy of **42** in a tumor growth inhibition (TGI) study using a human melanoma (A2058)[19] as the mouse xenograft model.

This tumor growth inhibition experiment employed daily oral administration of various inhibitor doses over 14 days in order to access the potential of the compound to function as an oral therapeutic agent (Figure 9). In this experiment, compound **42** demonstrated dose-dependent inhibition of tumor growth with >50% reduction observed with most doses (Figure 9A). For comparison, **1c** (Figure 1) was also administered in the same model at its maximum tolerated dose (MTD) (10 mg/kg) and displayed only 34% tumor reduction at this dose (Figure 9B). The 25 mg/kg dose of compound **42** was well tolerated, with no significant body weight loss (<10%) observed over the treatment period (Figure 10).

Table 3

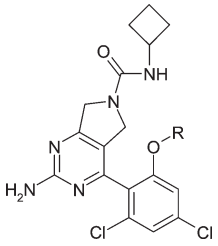

Compound#	R	Enzyme K_i[a] (μM)	Cell IC_{50}[b] (μM)	clogP	HLM CL_{int} (μL/min/mg)
16	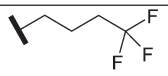	0.015	0.18	3.6	55.3
17	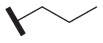	0.11	5.3	3.5	28
18	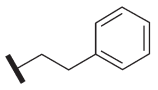	0.007	0.57	4.6	112
19	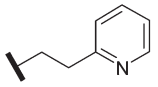	0.027	8	3.1	115
20	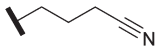	0.04	1.65	2.3	<8
21	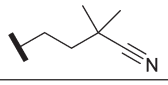	0.30	1.90	3	37.3
22	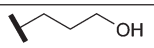	0.19	13	2	<8
23	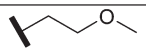	0.12	2	2.4	19.4
24	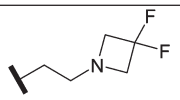	0.016	0.44	3.9	213
25	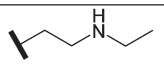	0.25	18%@ 10 μM	2.5	22.5
26	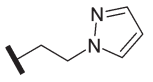	0.007	0.16	2.6	48

[a] Enzymatic K_i was calculated from enzymatic IC_{50} using the Cheng−Prusoff equation. Assay error is 10−15%. [b] Assay error is 10−15%. [c] CL_{int} is intrinsic clearance.

These results demonstrated a superior antitumor efficacy of **42** in this human melanoma model relative to **1c**. In addition, the converted survival study (Figure 11) confirmed that two mice dosed with compound **42** were tumor-free at the end of the study (120 days after the last dose of 25 mg/kg).

CHEMISTRY

The syntheses of compounds **7** and **8** are reported in the literature.[26] The syntheses of compounds **9**, **10**, and **11** are described in the Supporting Information. The amines required for the preparation of compounds **32**[27] and **33**[28] were prepared using literature methods.

The pyrrolodinopyrimidine-containing Hsp90 inhibitors described in this study were prepared using the methods described in Schemes 2−5. The starting materials used for these syntheses were **45** or **46** and their syntheses are described in Scheme 1. In Scheme 1, compound **43** was synthesized by following the known literature procedure.[29] Cyclization of **43** with guanidine carbonate gave compound **44** in reasonable yield. Subsequent chlorination using phosphorus oxychloride ($POCl_3$) provided compound **45** in reasonable yield. Removal of the ethyl carbamate present in **45** using a strong Lewis acid (iodotrimethylsilane, TMSI) also converted the associated 4-chloro atom to an iodide and gave **46** as the hydrogen iodide salt. We then developed several ways to synthesize the desired 2-amino-5,7-dihydro-6*H*-pyrrolo[3,4-*d*]pyrimidine-containing Hsp90 inhibitors starting from either **45** or **46**.

In Scheme 2, compound **46** was coupled with either commercially available isocyanates or various amines in the presence of 1,1-carbonyldiimidazole (CDI)[30] to form different urea moieties (intermediates **47a**−**e**). This CDI-mediated reaction successfully derivatized the pyrroloamino group present in **46** without simultaneously modifying the exocyclic amino group of the pyrimidine ring.

dx.doi.org/10.1021/jm200128m |*J. Med. Chem.* 2011, 54, 3368–3385

Table 4

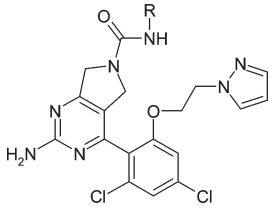

Compound#	R	Enzyme K_i[a] (μM)	Cell IC_{50}[b] (μM)	clogP	HLM CL_{int}[c] (μL/min/mg)	CACO-2 AB ($x10^{-6}$ cm/sec)
26		0.007	0.15	2.6	48	4.7
27	H	0.035	4.3	0.12	12	ND
28		0.02	0.54	1.7	<8	ND
29		0.013	0.49	2.1	12	ND
30		0.012	0.15	2.2	<8	0.5
31	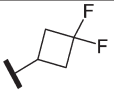	0.009	0.20	2	21	1.5
32		0.006	0.075	2.3	23	5
33	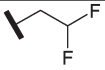	0.009	0.091	2	<8	1.2
34	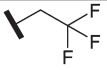	0.007	0.12	2.4	<8	0.96
35	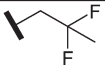	0.011	0.18	2.4	<8	1.2

[a] Enzymatic K_i was calculated from enzymatic IC_{50} using the Cheng−Prusoff equation. Assay error is 10−15%. [b] Assay error is 10−15%. [c] CL_{int} is intrinsic clearance.

Subsequent Suzuki coupling using 2,4,6-trisubstituted phenylboronic acid (**61**) and employing 1,4-dioxane as the solvent gave intermediates **48a**−**e** in good yields. Performing these coupling reactions using other solvents (e.g., acetonitrile, DMF, and DMSO) gave lower yields compared with 1,4-dioxane. Alkylation of **48a**−**e** with 1-iodo-4,4,4-trifluorobutane in the presence of Cs_2CO_3 then gave compounds **12**−**16** in good yield. The phenol present in **48e** was also alkylated using a variety of electrophiles to give compounds **16**−**23** (Scheme 3).

In Scheme 4, Suzuki coupling of compound **45** with boronic acid **61** provided intermediate **49** in good yield. Subsequent alkylation of **49** with 1-(2-bromoethyl)-1*H*-pyrazole[31] afforded compound **50**. The ethyl carbamate group present in **50** was deprotected using TMSI to give compound **51** as the corresponding hydrogen iodide salt. Compound **51** was then reacted with CDI and either 2,2,2-trifluoroethylamine or 2,2-difluoropropylamine[28] to form the urea-containing compounds **34** and **35**, respectively.

An alternative and more convergent synthesis is depicted in Scheme 5. The pyrroloamino group present in **46** was protected as a *tert*-butyl carbamate (compound **52**). This compound was then coupled with 2,4,6-trisubstituted boronic acids **61** and **63** to give compounds **53** and **54** in reasonable yields. The phenol moiety present in both **53** and **54** was derivatized using several pyrazole-containing alkylating agents (1-(2-bromoethyl)-1*H*-pyrazole[31] and **65**) to give intermediates **55**−**57**. The *tert*-butyl carbamate protecting group was subsequently removed from these molecules, and the resulting pyrroloamines (**58**−**60**) were transformed to the corresponding ureas (**26**−**35**, **38**−**42**) via CDI-mediated coupling with a variety of amines.

CONCLUSION

In summary, novel, potent, metabolically stable, and orally bioavailable non-quinone-containing Hsp90 inhibitors were identified from an HTS lead. Analysis of multiple X-ray cocrystal structures enabled the design and optimization of a novel class of 2-amino-5,7-dihydro-6H-pyrrolo[3,4-*d*]pyrimidine-containing compounds. The ligand lipophilicity efficiency (LipE) of the initial lead was improved considerably during the course of these optimization activities (3.34 increased to >5.50). These efforts culminated with the identification of compound **42** which

dx.doi.org/10.1021/jm200128m |*J. Med. Chem.* 2011, 54, 3368–3385

Table 5

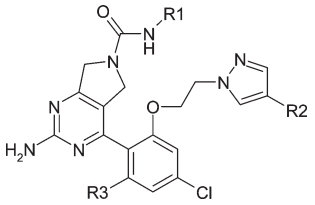

Compound#	R1	R2	R3	Cell IC_{50}[a] (μM)	HLM CL_{int} (unbound clearnce)[b] (μL/min/mg)	Human Cyp3A4 IC_{50}[c] (μM) (TI)[d]	IKr (μM) (TI)[d]
32		H	Cl	0.075	23 (115)	1.1 (15)	33.8 (450)
34	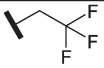	H	Cl	0.12	<8 (26)	1.9 (15)	105 (854)
35	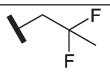	H	Cl	0.18	<8 (25)	3.3 (18)	147 (782)
36		CH_3	Cl	0.72	247	ND	ND
37		Cl	Cl	0.040	52	ND	ND
38		F	Cl	0.020	25 (154)	ND	ND
39	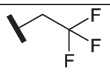	F	Cl	0.045	<8 (28)	0.8 (17)	62 (1377)
40	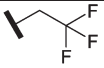	F	CH_3	0.037	9.7 (25)	1.4 (38)	228 (6162)
41	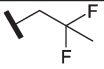	F	Cl	0.033	<8 (26)	0.6 (18)	70 (212)
42	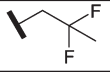	F	CH_3	0.036	<11 (27)	4.7 (131)	247 (6861)

[a] Assay error is <20%. [b] Unbound plasma clearance calculated based on human plasma protein binding. CL_{int} is intrinsic clearance. [c] CEREP bioprint assay; 7-benzyloxy-4-trifluoromethylcoumarin (BFC) was used as the substrate. [d] The rato between off-target activity IC_{50} and cell potency.

displayed good efficacy in a melanoma A2058 tumor model, exhibited expected pharmacodynamic effects in vivo, and possessed many other desirable pharmaceutical properties (e.g., high crystallinity and good solubility). The attractive attributes of **42** warranted its further examination for the treatment of cancer, and these studies will be reported in due course.

EXPERIMENTAL SECTION

Scintillation Proximity Assay (SPA). The ability of compounds to compete with a tritium labeled ligand for binding to N-terminus human Hsp90α was determined. The resultant IC_{50} is then used to calculate the K_i by using the Cheng−Prusoff equation. Chemical structure for this tritium labeled ligand and details relating to the SPA assay can be found in the Supporting Information.

Client Protein Degradation and Cell Growth Inhibition Assays. Primary cell assay IC_{50} was determined by the degradation of Akt in the non-small-cell lung carcinoma cell line NCI-H1299 as described previously.[18] The PD effects of Hsp90 inhibitors were measured by the

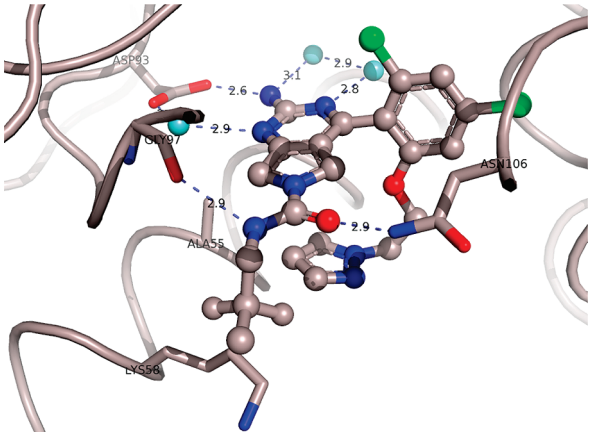

Figure 7. Crystal structure of **35** bound to the Hsp90 enzyme. The pyrazole moiety occupied the same space as the trifluoromethyl moiety present in compound **17** as shown in Figure 6.

dx.doi.org/10.1021/jm200128m |J. Med. Chem. 2011, 54, 3368–3385

Table 6. In Vitro Clearance, P450 Inhibition, Permeability, and Solubility Properties of 42

compd	liver microsome CL (μL/min/mg) human	rat	dog	MDCK AB (10^{-6}, cm/s)	MDCK BA (10^{-6}, cm/s)	Cyp enzymes,[a] IC_{50} (μM)	solubility (μM)
42	15	43	9.6	2.4	11	>30	200

[a] 1A2, 2B6, 2C8, 2C9, 2C19, 2D6, 3A4.

Table 7. In Vivo Pharmacokinetic Parameters of 42

species	dose (mg/kg)	route	CL_{plasma} (mL/min/kg)	Vd_{ss} (L/kg)	$T_{1/2}$ (h)	F_{oral} (%)[c]
rat WH	2.5	iv	77	9.6	6.7	
	10	po			13[a]	19,[a] 15[b]
dog beagle	0.5	iv	8.4	8.0	17	
	0.5	po			16[a]	63,[a] 58[b]

[a] Solution formulation: 40% PEG400 in saline. [b] Suspension formulation: 0.5% MC. [c] F_{oral} (%) = $(dose_{iv})(AUC_{po})/[(dose_{po})(AUC_{iv})]$.

Table 8. In Vitro Antiproliferation IC_{50} of 42 in Various Human Cancer Lines

tumor type	melanoma				colorectal	prostate
cell line	A2058	MeWo[a]	A375	SK-MEL2	HT-29	LNCap
IC_{50} (nM)	20	206	40	5	3	30

[a] Wild type B-Raf.

client protein (Akt and Her2) degradation measured by Luminex technology and ELISA. The details relating to these two assays can be found in the Supporting Information.

Pharmacokinetics. Male Wistar Han rats (n = 2 per group) were given **42** intravenously at 2.5 mg/kg or orally at 10 mg/kg in PEG400/saline solution (3:7, v/v). Male beagle dogs (n = 2 per group) were also given **42** intravenously or orally at 0.5 mg/kg in PEG400/saline solution (3:7, v/v). Blood samples were collected from all animals at predetermined time points with the anticoagulant (K_2EDTA or K_3EDTA) and were then centrifuged. The resulting plasma samples were stored at approximately −20 °C until analysis. Liquid chromatography−tandem mass spectrometry (LC−MS/MS) was used for quantitative analysis, and pharmacokinetic parameters were calculated using a standard noncompartmental method (Watson LIMS, version 7.2, Thermo Fisher Scientific, MA).

Microsomal Stability Studies. Compounds (1 μM) were incubated at 37 °C for 45 min in a final volume of 200 μL of 100 mM potassium phosphate buffer (pH 7.4) containing pooled liver microsomes (0.8 mg/mL protein) and 2 mM NADPH. Reactions were initiated with the addition of NADPH following a 10 min preincubation. Aliquots of incubation samples were protein precipitated with cold methanol containing 0.1 μM buspirone (internal standard) and centrifuged, and supernatants were analyzed by LC−MS/MS. All incubations were performed in triplicate. In vitro intrinsic clearance (CL_{int}) was calculated from the half-life ($t_{1/2}$) of the parent drug disappearance, which was determined by the slope (k) of log−linear regression analysis from the concentration versus time profiles, i.e., $t_{1/2} = -\ln(2)/k$.

Human Plasma Binding Measurements. In vitro plasma protein bindings were determined by equilibrium dialysis technique using a 96-well Teflon dialysis chamber (HTDialysis LLC, Gales Ferry, CT) with a semipermeable membrane (Spectra/Por4, Spectrum, Laguna Hills, CA) with a 12000−14000 Da molecular mass cutoff. Compounds

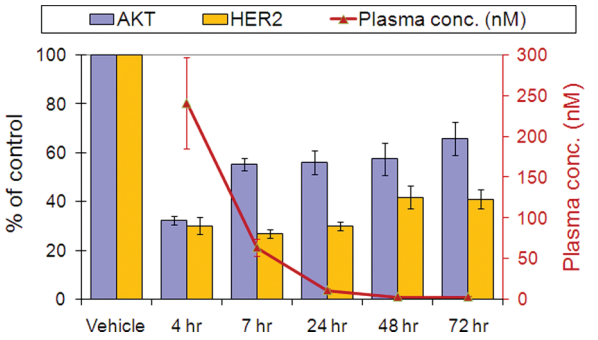

Figure 8. Relationship between in vivo biomarkers (Her and Akt) inhibition and plasma unbound concentration for **42**.

(1 μM) were incubated in plasma at 37 °C for 6 h. Appropriate volumes of plasma and buffer were protein-precipitated with cold acetonitrile and centrifuged, and supernatants were analyzed by LC−MS/MS. All incubations were performed in triplicate.

Efficacy Study in A2058 Melanoma Xenografts. Six- to eight-week-old nu/nu athymic female mice were obtained from The Jackson Laboratory and maintained in pressurized ventilated caging at the Pfizer La Jolla animal facility. All studies were done in compliance with Institutional Animal Care and Use Committees guidelines. Tumors were established by injecting 2 × 10^6 cells suspended 1:1 (v/v) with reconstituted basement membrane (Matrigel, BD Biosciences). Mice with established tumors of ∼150 mm^3 were selected and randomized, then orally treated with compound **42** once daily. Tumor dimensions were measured with vernier calipers, and tumor volumes were calculated using the formula of $(\pi/6)$(larger diameter)$(\text{smaller diameter})^2$. Tumor growth inhibition percentage (TGI %) was calculated as 100 × (1 − $\Delta T/\Delta C$). For the survival study, the dosing was stopped for all animals and measurement was performed 3 times/week, and the animals were sacrificed and noted "dead" when the tumor size reached 1500 mm^3. The survival study was performed for 120 days.

Chemistry. General Methods. All commercial reagents were used as received from their perspective supplier. The structures of the compounds of the following examples were confirmed by one or more of the following: proton magnetic resonance spectroscopy and liquid chromatography−mass spectrometry. Compound purity is determined by elemental microanalyses or high pressure liquid chromatography (HPLC) or high resolution mass spectrometry (HRMS). Proton magnetic resonance (^{1}H NMR) spectra were determined using either a Varian UNITY plus 300 or a Bruker 400. Chemical shifts are reported in parts per million (ppm, δ) downfield from an internal tetramethylsilane standard. Coupling constants are given in hertz. Flash column chromatography was performed using silica gel 60 (Merck Art 9385). Elemental microanalyses were performed by Atlantic Microlab Inc., Norcross, GA. HPLC conditions utilized are as follows: gradient, 5−95% B in 10 min, 95% B 10−12 min; flow rate 0.6 mL/min; column, Waters Acquity UPLC BEH C18, 1.7 μm, 2.1 mm × 100 mm; column temperature, 80 °C; mobile phase A, water (0.1% formic acid and 0.05% ammonium formate); mobile phase B, methanol (0.1%

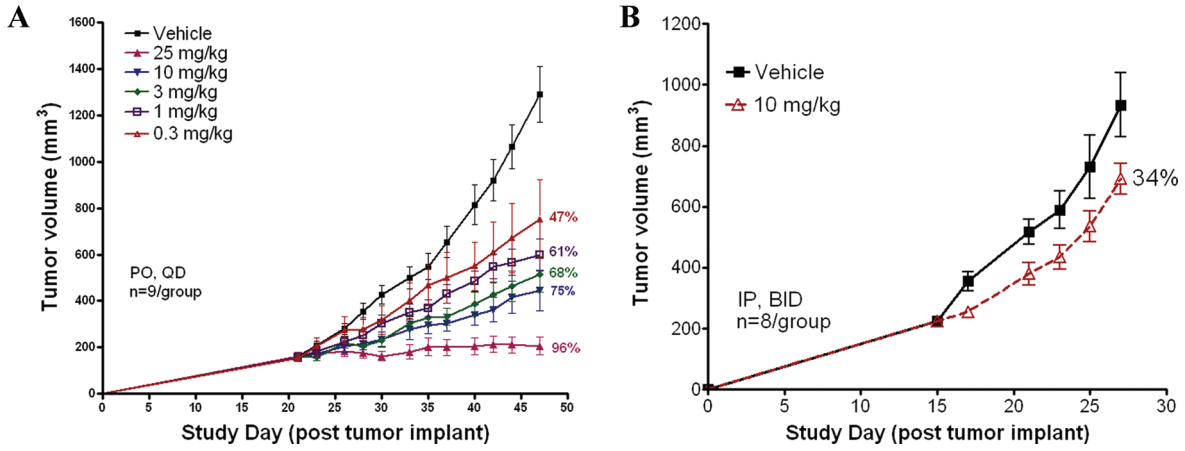

Figure 9. Tumor growth inhibition experiments of **42** (A) and **1c** (B) in A2058 model.

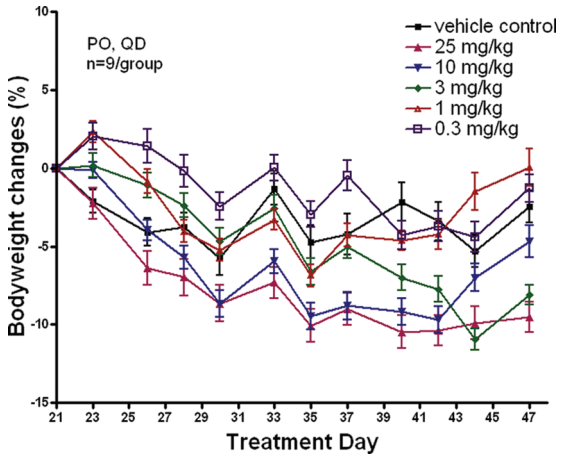

Figure 10. Body weight measurement during tumor growth inhibition experiment using **42**.

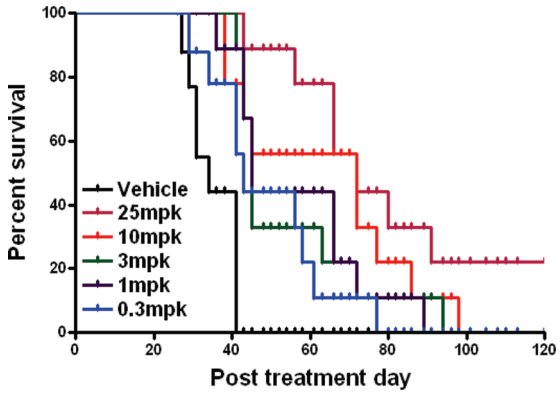

Figure 11. Compound **42** prolongs the survival of A2058 tumor-bearing animals.

formic acid and 0.05% ammonium formate); UV detector, 254 and 224 nm. Retention times (t_R) are in minutes, and purity is calculated as percent total area. Elemental microanalysis results of all final compounds were within ±0.4% of the theoretical values or were >95% pure by HPLC.

2-Amino-4-hydroxy-5,7-dihydropyrrolo[3,4-*d*]pyrimidine-6-carboxylic Acid Ethyl Ester (44). A 20 L vessel equipped with nitrogen inlet, condenser, temperature probe, and overhead stirrer was charged with 1408 g (6.14 mol) of **43**[29] and 11.5 L of *t*-BuOH. The mixture was stirred at 40−50 °C to give a clear orange solution. Then 1134 g (6.29 mol) of guanidine carbonate was added in one portion (strong evolution of gas was observed), and the orange-brown mixture was refluxed. More evolution of gas was observed. The mixture became somewhat darker, and some solid precipitated. The mixture was refluxed at 85 °C for 12 h. A beige suspension was obtained. The solution was adjust to pH 5 by adding 1 N HCl (aq). The milky solution was extracted with EtOAc. TLC (EtOAc/hexanes, 1:1) indicated that the starting material was consumed completely. Starting material was used as reference (R_f = 0.50 with tailing). The solvent was removed under reduced pressure to give a beige solid.

The material was suspended in 4.5 L of hot water and heated to 80 °C. Hydrochloric acid (30%, 575 mL) was added until pH was 7−6. The suspension was cooled to 0 °C and stirred for 2 h at 0 °C. The solid was collected and dried for 12 h. The light beige hard paste (about 2600 g) was transferred into a 20 L round-bottom flask for the large-scale rotavapor, and water was removed by stripping for five cycles with toluene (9 L) to give the title compound (996 g, 4.44 mol, 72%).

2-Amino-4-chloro-5,7-dihydropyrrolo[3,4-*d*]pyrimidine-6-carboxylic Acid Ethyl Ester (45). A 20 L reaction vessel, equipped with temperature probe, overhead stirrer, condenser, and nitrogen inlet, was charged with 9.5 L of CH_3CN. Compound **44** (990 g, 4.42 mol) was suspended in the solvent. Phosphorus oxychloride ($POCl_3$) (4.0 L, 43.7 mol) was added to this light beige suspension in 15 min. The internal temperature went up from 17 to 30 °C. The gray suspension was heated to reflux. Gas evolution was observed first, and the suspension became thicker. After 3 h of reflux, the internal temperature was 81 °C and the suspension had become somewhat browner and thinner. After 24 h of reflux the mixture was allowed to cool to room temperature. The volatiles were removed in vacuum, and the red-brown residue was dissolved in CH_3CN (2.5 L). The solvent was then removed in vacuum, and this was repeated one time with another 2.5 L of CH_3CN. All volatiles were removed in vacuum (16 mbar) to yield a red-brown foam. The red-brown foam was pulverized, and 4 L of water and 3 kg of ice were added. The red-brown suspension was stirred overnight at room temperature to destroy all remaining PO_xCl_y compounds. The red-brown suspension was cooled to 0 °C, and 30% NaOH (aq) was added slowly to pH 8, keeping the internal temperature below 12 °C. The

dx.doi.org/10.1021/jm200128m |*J. Med. Chem.* 2011, 54, 3368–3385

Scheme 1[a]

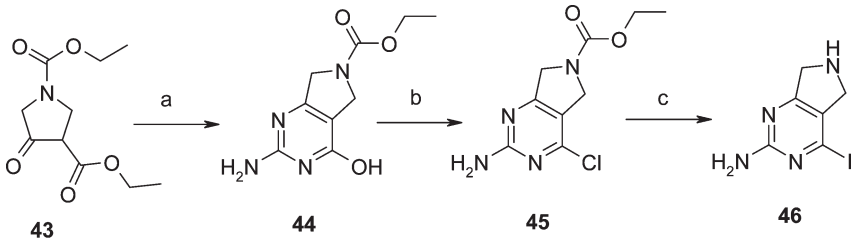

[a] Reagents and conditions: (a) guanidine carbonate, *t*-BuOH, 85 °C, 12 h, 52%; (b) $POCl_3$, CH_3CN, 81 °C, 3 h, 23%; (c) iodotrimethylsilane, CH_3CN, 81 °C, 4 h, 79%.

Scheme 2[a]

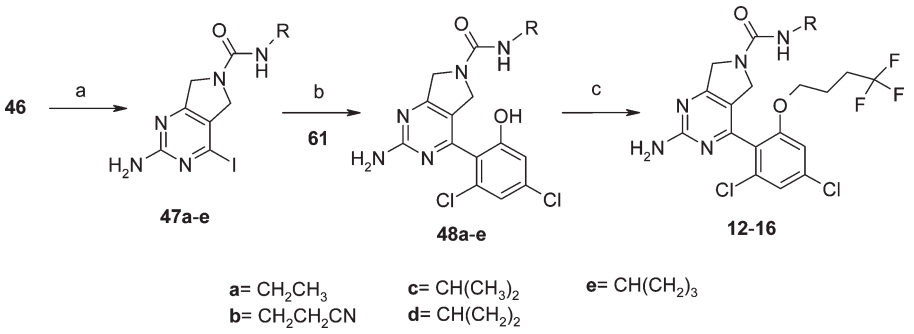

[a] Reagents and conditions: (a) isocyanates, DMSO, 23 °C, 3 h, or amines, CDI, THF, 23 °C, 3 h, 19−64%; (b) **61**, Na_2CO_3, $Pd(PPh_3)_4$, dioxane, 85 °C, 8 h; (c) 1-iodo-4,4,4-trifluorobutane, Cs_2CO_3, DMSO, 65 °C, 4 h, 36%.

Scheme 3[a]

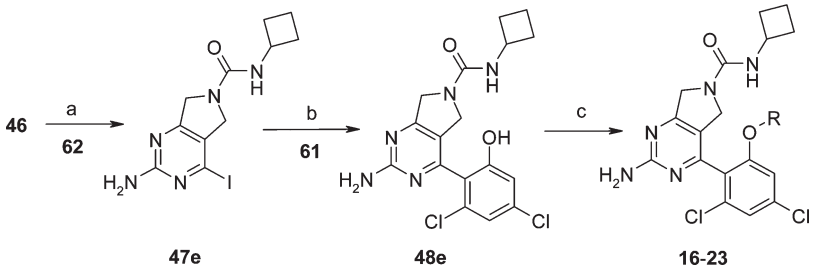

[a] Reagents and conditions: (a) **62**, Cs_2CO_3, DMSO, 50 °C, 1 h, 53.7%; (b) **61**, Na_2CO_3, $Pd(PPh_3)_4$, dioxane, 85 °C, 8 h; (c) alkylating agents, Cs_2CO_3, DMSO, 65 °C, 1 h, 23−51%.

Scheme 4[a]

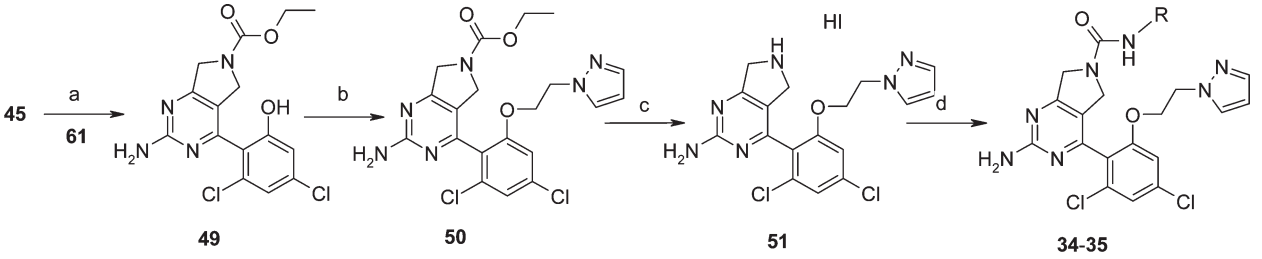

[a] Reagents and conditions: (a) **61**, $Pd(PPh_3)_4$, Na_2CO_3, 85 °C, 4.5 h, 76%; (b) 2-bromoethylpyrazole, K_2CO_3, DMSO, 55 °C, 1.5 h, 64%; (c) iodotrimethylsilane, $CHCl_3$, 23 °C, 24 h, 96%; (d) CDI, amines, THF, TEA, 60 °C, 4 h, 40−53%.

mixture became more yellow brownish. The suspension was stirred overnight at room temperature. The solid was collected and dried completely by evaporating with toluene (9 L) for four cycles. The light brown solid was purified by Soxhlet extraction with 1,4-dioxane to yield a light brown solid as the title compound 630 g (2.6 mol, 59%). ^{1}H NMR (400 MHz, DMSO-d_6) δ 4.45 (d, 4H); 4.10 (q, 2H); 1.24 (t, 3H). Anal. Calcd for $C_9H_{11}N_4O_2Cl \cdot 0.2\ H_2O$: C, 43.89%; H, 4.67%; N, 22.75%; Cl, 14.40%. Found: C, 44.06%; H, 4.63%; N, 22.43%; Cl, 14.35%.

dx.doi.org/10.1021/jm200128m |*J. Med. Chem.* 2011, 54, 3368–3385

Scheme 5[a]

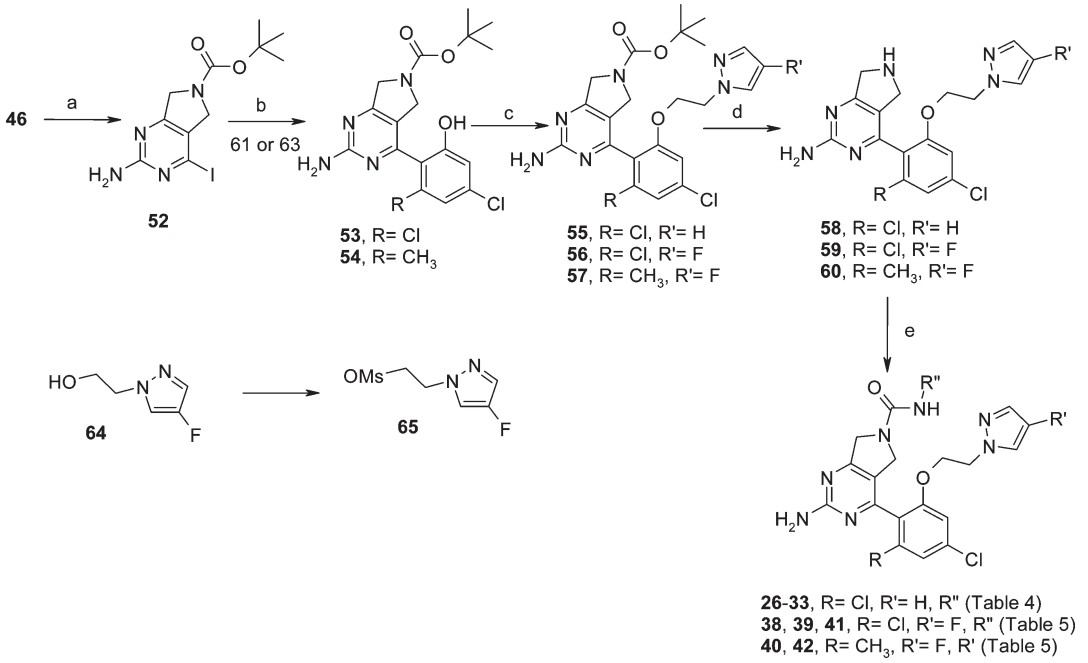

[a] Reagents and conditions: (a) di-*tert*-butyl dicarbonate, DIPEA, H_2O/dioxane, 23 °C, 1.5 h, 22%; (b) **61**/**63**, Na_2CO_3, $Pd(PPh_3)_4$, dioxane, microwave 120 °C, 40 min, 38%/60%; (c) bromoethylpyrazole/**65**, Cs_2CO_3/K_2CO_3, DMF, 70−100 °C, 1−2 h, 60−67%; (d) HCl (in dioxane, 4 M), 23 °C, 1−3 h; (e) CDI, amines, THF, TEA, 60 °C, 2 h, 27−59% (**26**−**33**) and 52−95.6% (**38**−**42**).

4-Iodo-6,7-dihydro-5*H*-pyrrolo[3,4-*d*]pyrimidin-2-ylamine (46). Iodotrimethylsilane (100 mL, 703 mmol) was added to a suspension of **45** (30.6 g, 126 mmol) in acetonitrile (750 mL). The resulting reaction mixture was heated at reflux for 4 h. After cooling to ambient temperature, the reaction mixture was quenched with MeOH (27 mL) and concentrated to dryness in vacuo. Traces of MeOH were removed via coevaporation with toluene (150 mL). The resulting residue was treated with Et_2O (200 mL), and the precipitate was filtered and washed with Et_2O. The crude brown powder was then stirred in refluxing EtOAc (250 mL) and cooled to ambient temperature. The resulting solid was collected by filtration and washed with more ethyl acetate to afford the desired product as a brown powder (52.2 g, 79%), which was used in the next step with further purification. ^{1}H NMR (400 MHz, DMSO-d_6) δ 4.25 (t, J = 5.1, 2H), 4.37 (t, J = 5.4, 2H), 9.41 (br s, 1H). MS: (M + H m/z) = 263.0.

2-Amino-4-iodo-5,7-dihydropyrrolo[3,4-*d*]pyrimidine-6-carboxylic Acid *tert*-Butyl Ester (52). Compound **46** (52.2 g, 100 mmol) was dissolved in dioxane (150 mL) and water (150 mL). Diisopropylethylamine (69.7 mL, 400 mmol) and di-*tert*-butyl dicarbonate (43.6 g, 200 mmol) were added to the solution, and the mixture was warmed to 45 °C. The mixture was then stirred at ambient temperature for an additional 1.5 h. The reaction mixture was poured into EtOAc (3.0 L) and saturated $NaHCO_3$ (aq) (1.0 L), and the mixture was stirred. The layers were separated, and the aqueous layer was washed once more with EtOAc (1.0 L). The combined organic layers were dried (Na_2SO_4), filtered, and concentrated in vacuo. The product was purified using a plug of silica gel and eluting with EtOAc (3 L) to give the title compound (8 g, 22%). ^{1}H NMR (400 MHz, $CDCl_3$-*d*) δ 5.17 (br s, 2H), 4.51−4.65 (m, 2H), 4.37−4.51 (m, 2H), 1.47−1.56 (m, 9H).

2-Amino-4-(2,4-dichloro-6-hydroxyphenyl)-5,7-dihydropyrrolo[3,4-*d*]pyrimidine-6-carboxylic Acid *tert*-Butyl Ester (53). Compound **61** (2.0 g, 2.76 mmol) was added to a suspension of **52** (1.0 g, 2.76 mmol) and sodium carbonate (3.0 mL, 2 M in H_2O) in dioxane (10 mL). The reaction mixture was purged with N_2 for 20 min. Then tetrakis(triphenylphosphine)palladium (319 mg, 0.28 mmol) was added. The resulting mixture was heated in a microwave at 120 °C for 40 min. After cooling to room temperature, the mixture was poured into H_2O (50 mL) and the aqueous solution was neutralized with HCl (1 N). EtOAc (3 × 100 mL) was added to extract the aqueous solution. The combined organic layer was dried, filtered, and concentrated to give a brown yellow oil. The product was purified by silica gel column and eluted at 60−70% EtOAc in hexanes to afford the title compound (419 mg, 38%). ^{1}H NMR (400 MHz, DMSO-d_6) δ 10.6 (br s, 1 H), 7.14 (s, 1 H), 6.97 (d, J = 2.0, 1 H), 6.79 (s, 2 H), 4.44 (d, J = 7.6, 2 H), 4.09−4.24 (m, 2 H), 1.43 (d, 9 H, two rotamer peaks). MS: (M + H m/z) = 398. Anal. Calcd for $C_{17}H_{18}Cl_2N_4O_3 \cdot 0.14$EtOAc: C, 51.49; H, 4.71; N, 13.68. Found: C, 51.51; H, 4.83; N, 13.42.

2-Amino-4-[2,4-dichloro-6-(2-pyrazol-1-ylethoxy)phenyl]-5,7-dihydropyrrolo[3,4-*d*]pyrimidine-6-carboxylic Acid *tert*-Butyl Ester (55). 1-(2-Bromoethyl)-1*H*-pyrazole (220 mg, 1.3 mmol) was added to a solution of **53** (250 mg, 0.63 mmol) and Cs_2CO_3 (615 mg, 1.89 mmol) in DMSO (6 mL). This mixture was heated at 70 °C for 2 h. After cooling to room temperature, the reaction mixture was partitioned between ethyl acetate (50 mL) and water (50 mL). The organic phase was separated, washed with water (1 × 50 mL) and brine (1 × 50 mL), dried over sodium sulfate, and concentrated to dryness. The desired product was purified by chromatography and eluted with 60−70% EtOAc in hexanes to afford the title compound as a solid (206 mg, 67% yield). MS: (M + H m/z) = 491.05.

4-[2,4-Dichloro-6-(2-pyrazol-1-ylethoxy)phenyl]-6,7-dihydro-5*H*-pyrrolo[3,4-*d*]pyrimidin-2-ylamine (58). A mixture of **55** (200 mg, 0.407 mmol) in 4 mL of TFA was stirred at room temperature for 3 h. After removal of excess TFA, the resulting residue was dissolved in a small amount of CH_3CN, neutralized with aqueous sodium bicarbonate, and concentrated to afford a solid, which was then suspended in ethyl

dx.doi.org/10.1021/jm200128m |*J. Med. Chem.* 2011, 54, 3368–3385

acetate and filtered. The resulting filtrate was concentrated to afford the title compound. MS: (M + H m/z) = 391.00.

2-Amino-4-[2,4-dichloro-6-(2-pyrazol-1-ylethoxy)phenyl]-5,7-dihydropyrrolo[3,4-*d*]pyrimidine-6-carboxylic Acid Cyclobutylamide (26). Cyclobutylamine (58 mg, 0.81 mmol) was added to a solution of 1,1-carbonyldiimidazole (132 mg, 0.81 mmol) in THF (2 mL) at 0 °C for 3 h. The resulting solution and TEA (0.17 mL, 1.2 mmol) were added to a solution of **58** (132 mg, 0.41 mmol) THF (2 mL). This reaction mixture was heated at 60 °C for 2 h. After concentration to dryness, the resulting residue was concentrated to dryness and purified by preparative HPLC to afford the title compound as a solid (104 mg, 52% yield over two steps). ^{1}H NMR (400 MHz, $CDCl_3$) δ ppm 7.45 (d, J = 1.3, 1 H), 7.15 (d, J = 1.5, 1 H), 7.02 (d, J = 1.8, 1 H), 6.86 (d, J = 1.5, 1 H), 6.12 (t, J = 1.8, 1 H), 5.29 (s, 2 H), 4.62 (s, 2 H), 4.33−4.47 (m, 4 H), 4.22−4.33 (m, 2 H), 4.13 (d, J = 12.4, 1 H), 3.75 (d, J = 11.4, 1 H), 2.31−2.48 (m, 2 H), 1.79−1.94 (m, 2 H), 1.65−1.78 (m, 2 H). MS: (M + H m/z) = 488.05; HRMS calcd for $C_{22}H_{24}Cl_2N_7O_2$ (M + H) 488.1363, found 488.1355, error = −1.72 ppm. Anal. Calcd for $C_{22}H_{23}Cl_2N_7O_2 \cdot 0.46H_2O$: C, 53.20; H, 4.85; N, 19.74; Found: C, 53.10; H, 4.81; N, 19.60. HPLC purity (254 nm): 99.0%. t_R = 11.452 min.

2-Amino-4-[2,4-dichloro-6-(2-pyrazol-1-ylethoxy)phenyl]-5,7-dihydropyrrolo[3,4-*d*]pyrimidine-6-carboxylic Acid Methylamide (28). Following the procedure for the preparation of **26** but substituting cyclobutylamine−CDI complex with methylamine provided the title compound in 44% yield. ^{1}H NMR (400 MHz, DMSO-d_6) δ 7.32 (d, J = 1.8, 1H), 7.29 (d, J = 1.5, 1H), 7.25 (d, J = 1.8, 1H), 7.19 (d, J = 2.0, 1H), 6.78 (br s, 2H), 6.18 (q, J = 4.3, 1H), 6.00 (t, J = 2.0, 1H), 4.30−4.45 (m, 6H), 3.92 (dd, J = 1.5, 12.6, 1H), 3.60 (d, J = 12.6, 1H), 2.59 (d, J = 4.3, 3H). MS: (M + H m/z) = 448.2. HRMS calcd for $C_{19}H_{19}Cl_2N_7O_2$ $[M + H]^+$ 448.1050, found 448.1053. HPLC purity (254 nM): 98.80%. t_R = 7.699 min.

2-Amino-4-[2,4-dichloro-6-(2-pyrazol-1-ylethoxy)phenyl]-5,7-dihydropyrrolo[3,4-*d*]pyrimidine-6-carboxylic Acid Amide (27). Trimethylsilyl isocyanate (21 mg, 0.15 mmol) was added to a solution of **58** (40 mg, 0.1 mmol) in 2-butanol (3 mL) at 23 °C. The mixture was stirred at 23 °C for 12 h. The solvent was evaporated and the residue was purified by reversed phase HPLC to provide the title compound (44 mg, 74%). ^{1}H NMR (400 MHz, DMSO-d_6) δ 7.32 (d, J = 1.8, 2H), 7.25 (d, J = 1.8, 1H), 7.19 (d, J = 2.0, 1H), 6.79 (s, 2H), 6.03 (t, J = 2.0, 1H), 5.91 (s, 2H), 4.39 (d, J = 4.6, 2H), 4.25−4.36 (m, 4H), 3.92 (d, J = 12.6, 1H), 3.62 (d, J = 13.1, 1H); MS: (M + H m/z) = 434.2. Anal. Calcd for $C_{20}H_{21}Cl_2N_7O_2 \cdot 0.75H_2O \cdot 0.25CH_3OH$: C, 48.09%; H, 4.31%; N, 21.51%. Found: C, 48.19%; H, 4.13%; N, 21.21%.

2-Amino-4-[2,4-dichloro-6-(2-pyrazol-1-ylethoxy)phenyl]-5,7-dihydropyrrolo[3,4-*d*]pyrimidine-6-carboxylic Acid Ethylamide (29). Following the procedure for the preparation of compound **28** but substituting methyl isocyanate with ethyl isocyanate provided the title compound in 27% yield. ^{1}H NMR (400 MHz, DMSO-d_6) δ 7.32 (d, J = 1.8, 1H), 7.29 (d, J = 1.3, 1H), 7.25 (d, J = 1.8, 1H), 7.19 (d, J = 1.8, 1H), 6.78 (s, 2H), 6.23 (t, J = 4.8, 1H), 6.00 (t, J = 2.0, 1H), 4.36−4.47 (m, 2H), 4.33 (s, 4H), 3.87−3.97 (m, 1H), 3.59 (d, J = 12.9, 1H), 2.98−3.14 (m, 2H), 1.02 (t, J = 7.2, 3H). MS: (M + H m/z) = 463.1. Anal. Calcd for $C_{20}H_{21}Cl_2N_7O_2 \cdot 0.75CH_3CO_2H \cdot 1.2H_2O$: C, 48.73%; H, 5.04%; N, 18.50%. Found: C, 48.63%; H, 4.68%; N, 18.20%.

2-Amino-4-[2,4-dichloro-6-(2-pyrazol-1-ylethoxy)phenyl]-5,7-dihydropyrrolo[3,4-*d*]pyrimidine-6-carboxylic Acid (2,2-Difluoroethyl)amide (33). Following the procedure for the preparation of **26** but substituting cyclobutylamine with 2,2-difluoroethylamine provided the title compound in 29% yield. ^{1}H NMR (400 MHz, DMSO-d_6) δ 7.32 (d, J = 1.8, 1H), 7.30 (d, J = 1.8, 1H), 7.26 (d, J = 1.8, 1H), 7.20 (d, J = 2.0, 1H), 6.80 (br s, 2H), 6.70 (br s, 1H), 6.00 (t, J = 2.0, 1H), 5.98 (tt, J = 56.3 and 4.0, 1H), 4.30−4.49 (m, 6H), 3.94 (d, J = 12.9, 1H), 3.56 (d, J = 12.6, 1H), 3.37−3.48 (m, 2H). MS: (M + H m/z) = 498.2. HRMS calcd for $C_{20}H_{19}Cl_2F_2N_7O_2$ $[M + H]^+$ 498.101 811, found 498.102 539. Anal. Calcd for $C_{20}H_{19}Cl_2F_2N_7O_2 \cdot 0.86H_2O$: C, 46.75%; H, 4.06%; N, 19.08%. Found: C, 46.83%; H, 4.02%; N, 18.95%.

2-Amino-4-[2,4-dichloro-6-(2-pyrazol-1-ylethoxy)phenyl]-5,7-dihydropyrrolo[3,4-*d*]pyrimidine-6-carboxylic Acid (3,3-Difluorocyclobutyl)amide (31). Following the procedure for the preparation of **26** but substituting cyclobutylamine with 3,3-difluorocyclobutylamine provided the title compound in 59% yield. ^{1}H NMR (400 MHz, DMSO-d_6) δ 7.32 (d, J = 1.8, 1H), 7.29 (d, J = 1.5, 1H), 7.26 (d, J = 1.5, 1H), 7.20 (d, J = 2.0, 1H), 6.77 (br s, 2H), 6.60 (d, J = 6.3, 1H), 6.00 (t, J = 2.0, 1H), 4.30−4.47 (m, 6H), 3.99−4.08 (m, 1H), 3.95 (d, J = 12.9, 1H), 3.60 (d, J = 12.9, 1H), 2.77−2.90 (m, 2H), 2.57−2.70 (m, 2H). MS: (M + H m/z) = 524.0. HRMS calcd for $C_{22}H_{21}Cl_2F_2N_7O_2$ $[M + H]^+$ 524.117 461, found 524.118 902. HPLC purity: t_R = 9.166, 99.20%. Anal. Calcd for $C_{22}H_{21}Cl_2F_2N_7O_2 \cdot 0.65H_2O$: C, 49.29%; H, 4.19%; N, 18.29%. Found: C, 49.45%; H, 4.19%; N, 17.91%.

2-Amino-4-[2,4-dichloro-6-(2-pyrazol-1-ylethoxy)phenyl]-5,7-dihydropyrrolo[3,4-*d*]pyrimidine-6-carboxylic Acid Bicyclo[1.1.1]pent-1-ylamide (32). Following the procedure for the preparation of **26** but substituting cyclobutylamine with bicyclo[1.1.1]pent-1-ylamine[27] provided the title compound in 49% yield. ^{1}H NMR (400 MHz, DMSO-d_6) δ 7.32 (d, J = 1.8, 1H), 7.30 (d, J = 1.8, 1H), 7.25 (d, J = 1.8, 1H), 7.19 (d, J = 2.0, 1H), 6.85 (br s, 1H), 6.78 (br s, 2H), 6.01 (t, J = 2.0, 1H), 4.29−4.44 (m, 6H), 3.89 (d, J = 12.9, 1H), 3.53 (d, J = 13.1, 1H), 2.35 (s, 1H), 1.95 (s, 6H). MS: (M + H m/z) = 500.2. HRMS calcd for $C_{23}H_{23}Cl_2N_7O_2$ $[M + H]^+$ 500.136 305, found 500.136 392. Anal. Calcd for $C_{23}H_{23}Cl_2N_7O_2 \cdot 0.94H_2O$: C, 53.40%; H, 4.85%; N, 18.95%. Found: C, 53.57%; H, 4.80%; N, 18.95%.

2-Amino-4-(4-chloro-2-hydroxy-6-methylphenyl)-5,7-dihydropyrrolo[3,4-*d*]pyrimidine-6-carboxylic Acid *tert*-Butyl Ester (54). Compound **63** (300 mg, 1.6 mmol) was added to a suspension of **52** (583 mg, 1.61 mmol) and sodium carbonate (2.4 mL, 2 M in H_2O) in dioxane (8 mL). The reaction mixture was purged with N_2 for 20 min. Then tetrakis(triphenylphosphine)palladium (116 mg, 0.1 mmol) was added. The resulting mixture was heated in a microwave at 120 °C for 40 min. After cooling to room temperature, the mixture was poured into H_2O (20 mL) and the aqueous solution was neutralized with HCl (1 N). EtOAc (3 × 30 mL) was added to extract the aqueous solution. The combined organic layer was dried, filtered, and concentrated to give a brown yellow oil. The product was purified by silica gel column and eluted at 60−70% EtOAc in hexanes to afford the title compound (361 mg, 59.6%). ^{1}H NMR (400 MHz, DMSO-d_6) δ 10.07 (s, 1H), 6.82 (s, 1H), 6.80 (s, 1H), 6.71 (s, 2H), 4.05−4.48 (m, 4H), 2.03 (s, 3H), 1.38−1.46 (d, 9H, two rotamer peaks); MS: (M + H m/z) = 377.2.

2-(4-Fluoropyrazol-1-yl)ethanol (64). Sodium hydride (13.8 g, 0.35 mol) was added to a solution of 4-fluoro-1*H*-pyrazole[32] (20 g, 0.23 mol) in DMF (200 mL) at 0 °C. The mixture was stirred at 23 °C for 1 h, and then 2-bromoethanol (43 g, 0.35 mol) was added dropwise at 0 °C. The resulting mixture was stirred at 40 °C for 12 h. TLC (petroleum ether/EtOAc = 1:1) indicated the reaction was complete. The mixture was partitioned between H_2O (1 L) and ethyl ether (1 L). The aqueous solution was extracted with more ethyl ether (4 × 1 L). The combined organic layer was dried, filtered, and concentrated to provide the title compound as a yellow oil (20 g, 66%).

Methanesulfonic Acid 2-(4-Fluoropyrazol-1-yl)ethyl Ester (65). Methylsulfonyl chloride (0.44 mL, 5.6 mmol) was added to a solution of **64** (500 mg, 3.75 mmol), 4-dimethylaminopyridine (46 mg, 0.38 mmol), and DIPEA (1.3 mL, 7.5 mmol) in DCM (10 mL) at 0 °C. The mixture was stirred at room temperature for 12 h. The mixture was poured into H_2O (40 mL), and the aqueous solution was extracted with EtOAc (3 × 30 mL). The combined organic layer was dried, filtered, and concentrated to give the title compound as a brown yellow oil. This compound was used for the next step reaction without further purification.

2-Amino-4-(4-chloro-2-hydroxy-6-methylphenyl)-5,7-dihydropyrrolo[3,4-*d*]pyrimidine-6-carboxylic Acid *tert*-Butyl Ester (57). Compound **65** (116 mg, 0.6 mmol) was added to a solution of **54** (84 mg, 0.22 mmol) and K_2CO_3 (154 mg, 1.2 mmol) in DMF (3 mL) at 23 °C under N_2. The reaction mixture was heated at 100 °C for 1 h. The mixture was poured into H_2O (20 mL), and the aqueous solution was extracted with EtOAc (3 × 50 mL). The combined organic layer was dried, filtered, and concentrated to give the product as a brown yellow oil. The product was purified by silica gel column and eluted at 90−100% EtOAc in hexanes to afford the title compound (66 mg, 60%). ^{1}H NMR (400 MHz, DMSO-d_6) δ 7.42 (dd, J = 4.4, 10.7, 1H), 7.28 (dd, J = 4.3, 18.4, 1H), 7.04 (s, 1H), 6.99 (s, 1H), 6.70 (s, 2H), 4.33−4.41 (m, 2H), 4.17−4.31 (m, 4H), 3.83 (dd, J = 12.9, 25.5, 1H), 3.50 (dd, J = 13.4, 23.5, 1H), 2.00 (s, 3H), 1.44 (d, 9H, two rotamer peaks). Anal. Calcd for $C_{23}H_{26}N_6O_3ClF \cdot 0.25CH_3CO_2C_2H_5 \cdot 0.5H_2O$: C, 55.44%; H, 5.62%; N, 16.16%. Found: C, 55.78%; H, 5.49%; N, 15.93%.

4-(4-Chloro-2-{2-[*N*-((*E*)-2-fluoro-propenyl)-*N*′-methyl-enehydrazino]ethoxy}-6-methylphenyl)-6,7-dihydro-5*H*-pyrrolo[3,4-*d*]pyrimidin-2-ylamine (60). Hydrogen chloride (5 mL, 4 M in dioxane, 20.5 mmol) was added to **57** (500 mg, 1 mmol) in methanol. The mixture was stirred at 23 °C for 12 h. The solvent was evaporated to give the title compound as a light yellow solid residue. This compound was used for the next step reaction without further purification.

2-Amino-4-{4-chloro-2-[2-(4-fluoropyrazol-1-yl)ethoxy]-6-methylphenyl}-5,7-dihydropyrrolo[3,4-*d*]pyrimidine-6-carboxylic Acid (2,2-Difluoropropyl)amide (42). Triethylamine (1.5 mL, 3.5 mmol) was added to a solution of 2,2-difluoropropylamine hydrochloride[28] (250 mg, 1.8 mmol) and 1,1′-carbonyldiimidazole (340 mg, 2.1 mmol) in DMF (15 mL). The solution was stirred at 23 °C for 12 h. The resulting solution and DIPEA (1.5 mL) were added to a solution of **60** (397 mg, 1 mmol), and the mixture was heated at 75 °C for 2 h. The reaction mixture was poured into H_2O (20 mL) and extracted with EtOAc (2 × 50 mL). The combined organic layer was dried, filtered, and concentrated to give a brown yellow oil. The desired product was purified by chromatography and eluted at 0−10% methanol in EtOAc to afford the title compound as a white solid (497 mg, 95.6%). ^{1}H NMR (400 MHz, DMSO-d_6) δ 7.36 (d, J = 4.6, 1H), 7.26 (d, J = 4.0, 1H), 7.05 (s, 1H), 7.00 (d, J = 1.3, 1H), 6.70 (s, 2H), 6.65 (s, 1H), 4.40 (s, 2H), 4.20−4.31 (m, 4H), 3.92 (d, J = 12.9, 1H), 3.65 (d, J = 12.9, 1H), 3.37−3.52 (m, 2H), 2.01 (s, 3H), 1.55 (t, J = 19.0, 3H). Anal. Calcd for $C_{22}H_{23}N_7O_2ClF_3 \cdot 0.25H_2O$: C, 51.37%; H, 4.60%; N, 19.06%. Found: C, 51.34%; H, 4.65%; N, 18.70%.

2-Amino-4-{2,4-dichloro-6-[2-(4-fluoropyrazol-1-yl)ethoxy]phenyl}-5,7-dihydropyrrolo[3,4-*d*]pyrimidine-6-carboxylic Acid Bicyclo[1.1.1]pent-1-ylamide (38). Following the procedure for the preparation of **26** but substituting cyclobutylamine with bicyclo[1.1.1]pent-1-ylamine[27] and bromoethylpyrazole with **65** provided the title compound in 72% yield. ^{1}H NMR (400 MHz, DMSO-d_6) δ 7.36 (d, J = 4.6, 1H), 7.34 (d, J = 1.8, 1H), 7.23−7.29 (m, 2H), 6.89 (br s, 1H), 6.79 (s, 2H), 4.30−4.43 (m, 4H), 4.20−4.28 (m, 2H), 3.93 (d, J = 13.1, 1H), 3.65 (d, J = 13.1, 1H), 2.34 (s, 1H), 1.94 (s, 6H). Anal. Calcd for $C_{23}H_{22}N_7O_2Cl_2F \cdot 1.0H_2O$: C, 51.50%; H, 4.51%; N, 18.28%. Found: C, 51.81%; H, 4.34%; N, 18.02%.

2-Amino-4-{2,4-dichloro-6-[2-(4-fluoropyrazol-1-yl)ethoxy]phenyl}-5,7-dihydropyrrolo[3,4-*d*]pyrimidine-6-carboxylic Acid (2,2,2-Trifluoroethyl)amide (39). Following the procedure for the preparation of **38** but substituting 2,2-difluoropropylamine with 2,2,2-trifluoroethylamine provided the title compound in 82% yield. ^{1}H NMR (400 MHz, DMSO-d_6) δ 7.37 (d, J = 4.6, 1H), 7.34 (d, J = 1.8, 1H), 7.28 (d, J = 1.5, 1H), 7.24 (d, J = 4.3, 1H), 6.97 (s, 1H), 6.82 (s, 2H), 4.40−4.45 (m, 2H), 4.31−4.38 (m, 2H), 4.20−4.28 (m, 2H), 3.99 (d, J = 12.6, 1H), 3.77−3.87 (m, 2H), 3.68 (d, J = 13.1, 1H). Anal. Calcd for $C_{20}H_{17}N_7O_2Cl_2F_4$: C, 44.96%; H, 3.21%; N, 18.35%. Found: C, 44.71%; H, 3.26%; N, 18.03%.

2-Amino-4-{4-chloro-2-[2-(4-fluoropyrazol-1-yl)ethoxy]-6-methylphenyl}-5,7-dihydropyrrolo[3,4-*d*]pyrimidine-6-carboxylic Acid (2,2,2-Trifluoroethyl)amide (40). Following the procedure for the preparation of **42** but substituting 2,2-difluoropropylamine with 2,2,2-trifluoroethylamine provided the title compound in 82% yield. ^{1}H NMR (400 MHz, DMSO-d_6) δ 7.37 (d, J = 4.3, 1H), 7.23 (d, J = 4.0, 1H), 7.06 (s, 1H), 7.01 (d, J = 1.3, 1H), 6.90 (s, 1H), 6.72 (s, 2H), 4.40 (s, 2H), 4.26 (dd, J = 3.8, 12.9, 4H), 3.91 (d, J = 12.6, 1H), 3.76−3.86 (m, 2H), 3.61 (d, J = 13.1, 1H), 2.01 (s, 3H). Anal. Calcd for $C_{21}H_{20}N_7O_2ClF_4$: C, 49.08%; H, 3.92%; N, 19.08%. Found: C, 48.82%; H, 3.99%; N, 18.89%.

2-Amino-4-{2,4-dichloro-6-[2-(4-fluoropyrazol-1-yl)ethoxy]phenyl}-5,7-dihydropyrrolo[3,4-*d*]pyrimidine-6-carboxylic Acid (2,2-Difluoropropyl)amide (41). Following the procedure for the preparation of **38** but substituting 2,2,2-trifluoroethylamine with 2,2-difluoropropylamine provided the title compound in 33% yield. ^{1}H NMR (400 MHz, DMSO-d_6) δ 7.36 (d, J = 4.8, 1H), 7.34 (d, J = 1.8, 1H), 7.28 (d, J = 1.8, 1H), 7.26 (d, J = 4.3, 1H), 6.81 (s, 2H), 6.69 (s, 1H), 4.40−4.47 (m, 2H), 4.31−4.37 (m, 2H), 4.20−4.28 (m, 2H), 4.00 (d, J = 12.9, 1H), 3.69 (d, J = 13.1, 1H), 3.43−3.55 (m, 2H), 1.56 (t, J = 19.0, 3H). Anal. Calcd for $C_{21}H_{20}N_7O_2Cl_2F_3 \cdot 1.75H_2O$: C, 44.89%; H, 4.22%; N, 17.45%. Found: C, 45.22%; H, 3.90%; N, 17.12%.

2-Amino-4-iodo-5,7-dihydropyrrolo[3,4-*d*]pyrimidine-6-carboxylic Acid Isopropylamide (47c). Isopropyl isocyanate (19.0 mg, 0.223 mmol) was added to a solution of **46** (103 mg, 0.199 mmol) and sodium carbonate (51.2 mg, 0.483 mmol)) in DMSO (1.8 mL) at 65 °C. After 3 h, the mixture was filtered and purified by preparative HPLC to provide the title compound (44 mg, 64%). ^{1}H NMR (300 MHz, DMSO-d_6) δ 7.03 (br s, 2H), 6.15 (d, J = 7.7, 1H), 4.41 (s, 2H), 4.26 (s, 2H), 3.73−3.87 (m, 1H), 1.09 (d, J = 6.6, 6H). MS: (M + H m/z) = 348.2.

2-Amino-4-(2,4-dichloro-6-hydroxyphenyl)-5,7-dihydropyrrolo[3,4-*d*]pyrimidine-6-carboxylic Acid Isopropylamide (48c). Sodium carbonate (2 M, 0.45 mL, 0.90 mmol) was added to a solution of **61** (94 mg, 0.45 mmol) and **47c** (145 mg, 0.418 mmol) in 1,4-dioxane (6.0 mL). The reaction mixture was purged with N_2 for 20 min before $Pd(PPh_3)_4$ (152 mg, 0.132 mmol) was added. The reaction mixture was heated to 85 °C for 8 h, cooled to room temperature, and partitioned between EtOAc and H_2O. The EtOAc layer contained only impurities and was discarded. The aqueous layer was brought to pH 5 with 1 N KH_2PO_3 and was extracted with EtOAc/*i*-PrOH. The organics were concentrated to give the desired product as a pale tan powder which was used without further purification. MS: (M + H m/z) = 382.0.

2-Amino-4-[2,4-dichloro-6-(4,4,4-trifluorobutoxy)phenyl]-5,7-dihydropyrrolo[3,4-*d*]pyrimidine-6-carboxylic Acid Isopropylamide (14). 1-Iodo-4,4,4-trifluorobutane (75 mg, 0.32 mmol) was added to a solution of **48c** (69 mg, 0.18 mmol) and Cs_2CO_3 (192 mg, 0.589 mmol) in DMSO (1.5 mL). The mixture was heated at 65 °C for 1 h and filtered. Preparative HPLC provided the title compound as a white powder (29 mg, 32%). ^{1}H NMR (300 MHz, DMSO-d_6) δ 7.36 (d, J = 1.5, 1H), 7.31 (d, J = 1.3, 1H), 6.81 (br s, 2H), 6.04 (d, J = 7.7, 1H), 4.39 (br s, 2H), 4.05−4.15 (m, 4H), 3.69−3.84 (m, 1H), 2.02−2.20 (m, 2H), 1.68−1.83 (m, 2H), 1.05 (d, 6H). MS: (M + H m/z) = 492.2. HRMS calcd for $C_{20}H_{22}Cl_2F_3N_5O_2$ $[M + H]^+$ 492.1175, found 492.1189. HPLC purity (254 nm): 98.26%. t_R = 11.582 min.

Imidazole-1-carboxylic Acid Cyclobutylamide (62). Cyclobutylamine (1.00 g, 14.1 mmol, dissolved in THF (9.0 mL)) was added to a solution of 1,1-carbonyldiimidazole (3.54 g, 21.8 mmol) in THF (100 mL) at 0 °C dropwise over 10 min. The reaction mixture was allowed to warm to room temperature and was stirred for 2 h. The solvent was removed under reduced pressure, and the resulting oil was purified on silica gel, eluting with 0−10% MeOH/DCM to provide the title compound as a clear oil (2.11 g, 90.8%). ^{1}H NMR (300 MHz, $CDCl_3$) δ 8.12 (s, 1H), 7.36 (t, J = 1.4, 1H), 7.08 (s, 1H), 6.35 (d,

J = 6.2, 1H), 4.35−4.54 (m, 1H), 2.36−2.53 (m, 2H), 1.95−2.15 (m, 2H), 1.71−1.90 (m, 2H).

2-Amino-4-iodo-5,7-dihydropyrrolo[3,4-*d*]pyrimidine-6-carboxylic Acid Cyclobutylamide (47e). Compound **62** (329 mg, 1.99 mmol) was added to a solution of **46** (961 mg, 1.86 mmol) and cesium carbonate (604 mg, 1.85 mmol) in DMSO (4 mL). The mixture was heated to 50 °C. After 1 h, the reaction mixture was cooled to room temperature and filtered. Preparative HPLC provided the title compound as a white powder (358 mg, 53.7%). ^{1}H NMR (300 MHz, DMSO-d_6) δ 7.02 (br s, 2H), 6.60 (d, J = 7.7, 1H), 4.41 (s, 2H), 4.26 (s, 2H), 4.06−4.20 (m, 1H), 2.07−2.18 (m, 2H), 1.89−2.05 (m, 2H), 1.48−1.65 (m, 2H). MS: (M + H m/z) = 360.2.

2-Amino-4-(2,4-dichloro-6-hydroxyphenyl)-5,7-dihydropyrrolo[3,4-*d*]pyrimidine-6-carboxylic Acid Cyclobutylamide (48e). Sodium carbonate (2 M, 1.4 mL, 2.8 mmol) was added to a solution of **61** (310 mg, 1.50 mmol) and **47e** (489 mg, 1.36 mmol) in 1,4-dioxane (20 mL). The reaction mixture was purged with N_2 for 20 min before tetrakis(triphenylphosphine)palladium (152 mg, 0.132 mmol) was added. The reaction mixture was heated to 85 °C for 8 h, cooled to room temperature, and partitioned between EtOAc and H_2O. The EtOAc layer contained only impurities and was discarded. The aqueous layer was brought to pH 5 with 1 N KH_2PO_3 and was extracted with EtOAc/*i*-PrOH. The organics were concentrated to give the desired product as a pale tan powder which was used without further purification. ^{1}H NMR (300 MHz, DMSO-d_6) δ 10.64 (s, 1H), 7.15 (d, J = 1.3, 1H), 6.96 (d, J = 1.3, 1H), 6.80 (br s, 2H), 6.52 (d, J = 7.9, 1H), 4.40 (br s, 2H), 4.15 (m, 3H), 2.01−2.17 (m, 2H), 1.83−2.00 (m, 2H), 1.45−1.63 (m, 2H). MS: (M + H m/z) = 394.2.

2-Amino-4-[2,4-dichloro-6-(4,4,4-trifluorobutoxy)phenyl]-5,7-dihydropyrrolo[3,4-*d*]pyrimidine-6-carboxylic Acid Cyclobutylamide Hydrochloride (16). 1-Iodo-4,4,4-trifluorobutane (89.2 mg, 0.38 mmol) was added to a solution of **48e** (91.1 mg, 0.23 mmol) and Cs_2CO_3 (174 mg, 0.53 mmol) in DMSO (1.5 mL). The reaction mixture was heated to 65 °C for 30 min. The reaction mixture was cooled to 23 °C and filtered. Preparative HPLC provided the title compound as a white powder (46 mg, 37%). ^{1}H NMR (400 MHz, DMSO-d_6) δ 7.37 (d, J = 1.8, 1H), 7.31 (d, J = 1.8, 1H), 6.86 (br s, 2H), 6.51 (d, J = 7.3, 1H), 4.34−4.46 (m, 2H), 4.05−4.18 (m, 5H), 2.03−2.18 (m, 4H), 1.85−1.97 (m, 2H), 1.76 (quin, J = 7.0, 2H), 1.47−1.59 (m, 2H). MS: (M + H m/z) = 504.2. Anal. Calcd for $C_{21}H_{22}N_5O_2Cl_2 \cdot 1.0$HCl: C, 46.64%; H, 4.29%; N, 12.95%. Found: C, 46.75%; H, 4.26%; N, 12.69%.

2-Amino-4-(2,4-dichloro-6-hydroxyphenyl)-5,7-dihydropyrrolo[3,4-*d*]pyrimidine-6-carboxylic Acid Ethyl Ester (49). The reaction was performed under nitrogen. A 10 L reaction vessel, equipped with overhead stirrer, condenser, temperature probe, and nitrogen inlet, was charged with **45** (142.8 g, 588 mmol), **61** (120.6 g, 583 mmol, 0.99 equiv), $Pd(PPh_3)_4$ (46.7 g, 40.4 mmol, 6.9 mol %), and 1,4-dioxane (5 L). The mixture was bubbled with nitrogen for at least 30 min. Simultaneously, a solution of of $Na_2CO_{3(aq)}$ (187 g, 1.76 mol, 3.0 equiv, 820 mL) was bubbled with nitrogen for 30 min as well. The dioxane mixture was heated, and when the internal temperature was 50 °C, the Na_2CO_3 solution was added to the mixture. The mixture was heated at 84−86 °C for 4.5 h and then cooled to room temperature. The volatiles were removed in vacuum, and the orange-brown residue was mixed with $NaOH_{(aq)}$ (0.5 N, 10 L). The mixture was washed with TBME (3 × 2.5 L). The combined aqueous layers were acidified with KH_2PO_4/H_3PO_4 to pH 5−6. The water layer was extracted with EtOAc (6 × 3 L). The combined organics were dried over Na_2SO_4, filtered, and concentrated in vacuum to give an orange-yellow solid that was further purified in portions by Soxhlet extraction with a 3:1 mixture of TBME/EtOAc to give the product (165 g, 447 mmol, 76%). ^{1}H NMR (300 MHz, DMSO-d_6) δ 10.65 (br, 1H); 7.11 (s, 1H); 6.95 (s, 1H); 6.80 (s, 2H); 4.45 (d, 2H); 4.20 (m, 2H); 4.03 (2 q, 2H, rotamer A + B); 1.13 (2 t, 3H, rotamer A + B). HRMS calcd for $C_{15}H_{14}Cl_2N_4O_3$ 369.0516 $[M + H]^+$, found 369.0521.

2-Amino-4-[2,4-dichloro-6-(2-pyrazol-1-ylethoxy)phenyl]-5,7-dihydropyrrolo[3,4-*d*]pyrimidine-6-carboxylic Acid Ethyl Ester (50). The reaction was performed under nitrogen. A 1000 mL three-necked round-bottom flask was charged with **49** (57.78 g, 156.5 mmol), K_2CO_3 (343.3 g, 313 mmol, 2.0 equiv), and DMSO (650 mL). The mixture was heated to 55−56 °C. By syringe-pump, 1-(2-bromoethyl)-1*H*-pyrazole (738 g, 217 mmol, 1.4 equiv) was added in the course of 2.5 h. The orange-brown mixture was heated at 55−56 °C for an additional 1.5 h. The mixture was cooled to room temperature. The mixture was poured into 6 L of water and 7 L of toluene. The layers were separated, and the water layer was extracted with toluene (3 × 2 L). The combined toluene layers were washed with water (6 × 1 L) and dried over Na_2SO_4. After filtration the toluene was removed in vacuum. The crude product was dissolved in EtOAc (2 L) and filtered. The EtOAc was removed in vacuum to give 45 g of crude product. The crude product was stirred in toluene (50 mL) and the light yellow solid was collected, washed with toluene (3 × 20 mL), and dried by suction to give the title compound (46.5 g, 64%).

4-[2,4-Dichloro-6-(2-pyrazol-1-ylethoxy)phenyl]-6,7-dihydro-5*H*-pyrrolo[3,4-*d*]pyrimidin-2-ylamine (51). The synthesis and work-up were performed under a nitrogen atmosphere. A 1000 mL three-necked round-bottom flask equipped with temperature probe, reflux condenser, and nitrogen inlet was flushed with nitrogen and charged with **50** (64.5 g, 139.2 mmol) and chloroform (500 mL). Iodotrimethylsilane (114 g, 570 mmol, 4 equiv) was added to the brown solution. The temperature increased from 18 to 27 °C. The brown solution was refluxed for 24 h. The reaction mixture was cooled to 0 °C, and MeOH (200 mL) was added slowly to keep the internal temperature below 15 °C. A sticky, light colored, solid precipitated, and gas evolution was observed. The mixture was stirred at 10−15 °C to become a homogeneous brown solution. After 30 min of stirring, the volatiles were removed under reduced pressure, giving an orange-brown solid. The solid was stirred overnight in a mixture of 500 mL of diethyl ether and 200 mL of methanol. The suspension was filtered under a nitrogen atmosphere, and the beige solid was washed with more diethyl ether (3 × 200 mL). The solid under reduced pressure gave the title compound (103.7 g, 96%). ^{1}H NMR (300 MHz, CD_3OD) δ 8.17 (d, J = 1.9, 1H); 8.03 (d, J = 2.5, 1H); 7.37 (d, J = 1.7, 1H); 7.34 (d, J = 1.7, 1H); 6.59 (t, J = 2.6, 1H); 5.1−4.9 (m, 8H); 4.85 (s, 1H); 4.79 (s, 1H); 4.71 (d, J = 14.9, 2H); 4.56 (d, J = 14.6, 2H).

2-Amino-4-[2,4-dichloro-6-(2-pyrazol-1-ylethoxy)phenyl]-5,7-dihydropyrrolo[3,4-*d*]pyrimidine-6-carboxylic Acid (2,2-Difluoropropyl)amide (35). Triethylamine (5.1 mL, 37 mmol) was added to a solution of 2,2-difluoropropylamine[27] (2.4 g, 18 mmol) and 1,1′-carbonyldiimidazole (4.6 g, 27.4 mmol) in DCM (80 mL). The solution was stirred at 23 °C for 12 h. The resulting solution and TEA (5 mL) were added to a solution of **51** (4.7 g, 6 mmol) in DMF (36 mL), and the mixture was heated at 60 °C for 4 h. The reaction mixture was poured into H_2O (20 mL) and extracted with EtOAc (2 × 50 mL). The combined organic layer was dried, filtered, and concentrated to give a brown yellow oil. The desired product was purified by chromatography and eluted with 0−10% methanol in DCM to afford the title compound as a white solid (1.7 g, 53%). ^{1}H NMR (400 MHz, DMSO-d_6) δ 7.33 (d, J = 1.8, 1H), 7.29 (d, J = 1.5, 1H), 7.27 (d, J = 1.8, 1H), 7.20 (d, J = 2.3, 1H), 6.82 (s, 2H), 6.67 (s, 1H), 6.00 (t, J = 2.0, 1H), 4.40−4.48 (m, 2H), 4.31−4.37 (m, 4H), 3.97 (d, J = 12.9, 1H), 3.54−3.63 (m, 1H), 3.41−3.54 (m, 2H), 1.57 (t, J = 19.1, 3H). Anal. Calcd for $C_{21}H_{21}N_7O_2Cl_2F_2$: C, 49.23%; H, 4.13%; N, 19.14%. Found: C, 48.95%; H, 4.21%; N, 18.76%.

2-Amino-4-[2,4-dichloro-6-(2-pyrazol-1-ylethoxy)phenyl]-5,7-dihydropyrrolo[3,4-*d*]pyrimidine-6-carboxylic Acid (2,2,2-Trifluoroethyl)amide (34). Following the procedure for the preparation of **35** but substituting 2,2-difluoropropylamine with 2,2,2-trifluoroethylamine provided the title compound in 40% yield. ^{1}H NMR (400 MHz, DMSO-d_6) δ 7.33 (d, J = 1.8, 1H), 7.27 (d, J = 1.5, 2H), 7.21 (d, J = 1.8, 1H), 6.82 (s, 2H), 5.98 (t, J = 2.0, 1H), 4.41−4.49 (m, 2H), 4.30−4.37 (m, 4H), 3.94 (d, J = 12.9, 1H), 3.85 (dd, J = 6.3, 9.4, 2H), 3.54 (d,

J = 12.4, 1H). Anal. Calcd for $C_{20}H_{18}N_7O_2Cl_2F_3 \cdot 0.5H_2O$: C, 45.73%; H, 3.65%; N, 18.66%. Found: C, 45.89%; H, 3.56%; N, 18.39%.

2-Amino-4-[2,4-dichloro-6-(2-pyrazol-1-ylethoxy)phenyl]-5,7-dihydropyrrolo[3,4-*d*]pyrimidine-6-carboxylic Acid Cyclopropylamide (30). Following the procedure for the preparation of **26** but substituting cyclobutylamine with cyclopropylamine provided the title compound in 43% yield. ^{1}H NMR (400 MHz, DMSO-d_6) δ 7.31 (d, J = 1.5, 1 H), 7.29 (d, J = 1.5, 1 H), 7.24 (d, J = 1.5, 1 H), 7.18 (d, J = 2.0, 1 H), 6.78 (s, 2 H), 6.34 (br s, 1 H), 6.00 (t, J = 1.9, 1 H), 4.35−4.45 (m, 2 H), 4.32 (s, 4 H), 3.85−3.93 (m, 1 H), 3.51−3.58 (m, 1 H), 2.52−2.57 (m, 1 H), 0.49−0.59 (m, 2 H), 0.34−0.44 (m, 2 H). MS: (M + H m/z) = 474.10. HRMS calcd for $C_{21}H_{22}Cl_2N_7O_2$ (M + H) 474.120655, found 474.119412, error = −2.62 ppm. Anal. Calcd for $C_{21}H_{21}Cl_2N_7O_2 \cdot 1.19H_2O \cdot 0.13$HOAc: C, 50.72%; H, 4.78%; N, 19.49%. Found: C, 50.79%; H, 4.56%; N, 19.38%. HPLC purity (254 nm): 98.0%. t_R = 8.451 min.

2-Amino-4-[2,4-dichloro-6-(4,4,4-trifluorobutoxy)phenyl]-5,7-dihydropyrrolo[3,4-*d*]pyrimidine-6-carboxylic Acid Ethylamide (12). Following the procedure for the preparation of compound **16** but substituting compound **62** with ethyl isocyanate provided the title compound in 52% yield. ^{1}H NMR (400 MHz, DMSO-d_6) δ 7.36 (d, J = 1.8, 1H), 7.30 (d, J = 1.8, 1H), 6.82 (s, 2H), 6.54 (s, 1H), 4.30−4.46 (m, 2H), 3.97−4.18 (m, 4H), 2.98−3.13 (m, 2H), 2.06−2.17 (m, 2H), 1.68−1.83 (m, 2H), 1.00 (t, J = 7.1, 3H). Anal. Calcd for $C_{19}H_{20}Cl_2F_3N_5O_2 \cdot 1.0H_2O$: C, 45.98%; H, 4.47%; N, 14.10%. Found: C, 45.75%; H, 4.16%; N, 13.85%.

2-Amino-4-[2,4-dichloro-6-(4,4,4-trifluorobutoxy)phenyl]-5,7-dihydropyrrolo[3,4-*d*]pyrimidine-6-carboxylic Acid Cyanomethylamide (13). Following the procedure for the preparation of compound **16** but substituting compound **62** with 3-aminopropionitrile provided the title compound in 10% overall yield from **46**. ^{1}H NMR (300 MHz, DMSO-d_6) δ 7.36 (d, J = 1.3, 1H), 7.31 (d, J = 1.5, 1H), 6.85 (br s, 2H), 6.81 (t, J = 5.5, 1H), 4.34−4.50 (m, 2H), 4.04−4.20 (m, 4H), 3.25 (q, J = 6.1, 2H), 2.62 (t, J = 6.3, 2H), 2.02−2.20 (m, 2H), 1.76 (quin, 2H). MS: (M + H m/z) = 503.2. HRMS calcd for $C_{20}H_{19}Cl_2F_3N_6O_2$ [M +H]$^+$ 503.09714, found 503.09674. HPLC purity (254 nm): 95.55%. t_R = 8.890 min.

2-Amino-4-[2,4-dichloro-6-(4,4,4-trifluorobutoxy)phenyl]-5,7-dihydropyrrolo[3,4-*d*]pyrimidine-6-carboxylic Acid Cyclopropylamide (15). Following the procedure for the preparation of compound **16** but substituting compound **62** with cyclopropylamine provided the title compound in 19% yield. ^{1}H NMR (400 MHz, CD_3OD) δ 7.23 (d, J = 1.8, 1H), 7.17 (d, J = 1.8, 1H), 4.48−4.54 (m, 2H), 4.21−4.33 (m, 2H), 4.01−4.15 (m, 2H), 2.51−2.61 (m, 1H), 2.00−2.23 (m, 2H), 1.80−1.93 (m, 2H), 0.60−0.71 (m, 2H), 0.43−0.53 (m, 2H). MS: (M + H m/z) = 490.2. HRMS calcd for $C_{20}H_{20}Cl_2F_3N_5O_2$ [M + H]$^+$ 490.1019, found 490.1029.

Amino-4-(2,4-dichloro-6-phenethyloxyphenyl)-5,7-dihydropyrrolo[3,4-*d*]pyrimidine-6-carboxylic Acid Cyclobutylamide (18). Following the procedure for the preparation of **16** but substituting 1-iodo-4,4,4-trifluorobutane with bromoethylbenzene provided the title compound in 24% yield. ^{1}H NMR (300 MHz, DMSO-d_6) δ 7.30 (s, 1H), 7.26 (s, 1H), 7.02−7.18 (m, 3H), 6.98 (d, J = 6.4, 2H), 6.83 (br s, 2H), 6.39 (d, J = 7.7, 1H), 4.34−4.46 (m, 2H), 4.07−4.33 (m, 3H), 3.94 (d, J = 12.2, 1H), 3.60 (d, J = 12.6, 1H), 2.69−2.92 (m, 2H), 2.03−2.18 (m, 2H), 1.83−2.02 (m, 2H), 1.45−1.63 (m, 2H). MS: (M + H m/z) = 498.10/500.05. HRMS calcd for $C_{25}H_{26}Cl_2N_5O_2$ (M + H) 499.1488, found 499.1502, error = 2.85 ppm. HPLC purity (254 nm): 98.1%. t_R = 11.795 min.

2-Amino-4-[2,4-dichloro-6-(3-cyano-3,3-dimethylpropoxy)phenyl]-5,7-dihydropyrrolo[3,4-*d*]pyrimidine-6-carboxylic Acid Cyclobutylamide (21). Following the procedure for the preparation of **16** but substituting 1-iodo-4,4,4-trifluorobutane with 4-bromo-2,2-dimethylbutyronitrile provided the title compound in 33% yield. ^{1}H NMR (300 MHz, DMSO-d_6) δ 7.38 (s, 1H), 7.37 (s, 1H), 6.80 (br s, 2H), 6.51 (d, J = 7.7, 1H), 4.30−4.46 (m, 2H), 4.05−4.24 (m, 5H), 2.01−2.15 (m, 2H), 1.79−2.00 (m, 4H), 1.53 (d, J = 4.5, 2H), 1.19 (d, 6H). MS: (M + H m/z) = 489.2. HRMS calcd for $C_{23}H_{26}Cl_2N_6O_2$ [M + H]$^+$ 489.156 706, found 489.156 383. HPLC purity (254 nm): 97.21%. t_R = 9.706 min.

2-Amino-4-[2,4-dichloro-6-(3-hydroxypropoxy)phenyl]-5,7-dihydropyrrolo[3,4-*d*]pyrimidine-6-carboxylic Acid Cyclobutylamide (22). Following the procedure for the preparation of **16** but substituting 1-iodo-4,4,4-trifluorobutane with 3-iodopropan-1-ol provided the title compound in 24% yield. ^{1}H NMR (300 MHz, DMSO-d_6) δ 7.32 (s, 1H), 7.28 (s, 1H), 6.82 (br s, 2H), 6.51 (d, J = 7.54 Hz, 1H), 4.41 (br s, 2H), 4.02−4.19 (m, 5H), 3.31 (t, J = 5.56 Hz, 2H), 2.02−2.15 (m, 2H), 1.93−1.99 (m, 2H), 1.62−1.74 (m, 2H), 1.45−1.60 (m, 2H). MS: (M + H m/z) = 452.2. HRMS calcd for $C_{20}H_{23}Cl_2N_5O_3$ [M + H]$^+$ 452.1251, found 452.1251. HPLC purity (254 nm): 95.13%. t_R 11.273 min.

2-Amino-4-[2,4-dichloro-6-(2-methoxyethoxy)phenyl]-5,7-dihydropyrrolo[3,4-*d*]pyrimidine-6-carboxylic Acid Cyclobutylamide (23). Following the procedure for the preparation of **16** but substituting 1-iodo-4,4,4-trifluorobutane with 1-bromo-2-methoxyethane provided the title compound in 23% yield. ^{1}H NMR (300 MHz, DMSO-d_6) δ 7.34 (d, J = 1.7, 1H), 7.31 (d, J = 1.5, 1H), 6.81 (br s, 2H), 6.49 (d, J = 8.1, 1H), 4.40 (br s, 2H), 4.05−4.23 (m, 5H), 3.45−3.52 (m, 2H), 3.12 (s, 3H), 2.02−2.15 (m, 2H), 1.83−1.99 (m, 2H), 1.46−1.60 (m, 2H). MS: (M + H m/z) = 452.0. HRMS calcd for $C_{20}H_{23}Cl_2N_5O_3$ [M + H]$^+$ 452.1251, found 452.1243. HPLC purity (254 nm): 98.53%. t_R = 9.524 min.

2-Amino-4-[2,4-dichloro-6-(2-pyridin-2-ylethoxy)phenyl]-5,7-dihydropyrrolo[3,4-*d*]pyrimidine-6-carboxylic Acid Cyclobutylamide (19). Diisopropyl azodicarboxylate (0.040 mL, 0.21 mmol) was added to a solution of **48e** (32 mg, 0.081 mmol), 2-pyridin-2-ylethanol (34 mg, 0.28 mmol), and triphenylphosphine (53 mg, 0.20 mmol) in THF (1.5 mL) at 0 °C. The mixture was stirred at 23 °C for 3 h, diluted with DMSO (1.5 mL), and then the THF was removed under vacuum. Preparative HPLC provided the title compound as an off white powder (20.8 mg, 51%). ^{1}H NMR (300 MHz, DMSO-d_6) δ 8.36 (d, J = 4.1, 1H), 7.50 (td, J = 1.8, 7.6, 1H), 7.30 (s, 2H), 6.99−7.07 (m, 1H), 6.91 (d, J = 7.7, 1H), 6.77 (br s, 2H), 6.37 (d, J = 8.1, 1H), 4.26−4.45 (m, 4H), 4.07−4.25 (m, 1H), 3.86 (d, J = 13.0, 1H), 2.91−3.04 (m, 2H), 2.05−2.21 (m, 2H), 1.85−2.03 (m, 2H), 1.47−1.64 (m, 2H). MS: (M + H m/z = 499.2). HRMS calcd for $C_{24}H_{24}Cl_2N_6O_2$ [M + H]$^+$ 499.1411, found 499.1411. HPLC purity (254 nm): 96.23%. t_R = 9.369 min.

■ ASSOCIATED CONTENT

Supporting Information. Experimental details and analytical data for **9**, **10**, **11**, **24**, **25**, **36**, **37**, **61**, and **63**, in vitro enzymatic competitive binding assay, cell assay, in vivo biologicals, and pharmacokinetic experiments. This material is available free of charge via the Internet at http://pubs.acs.org.

■ AUTHOR INFORMATION

Corresponding Author

*Phone: 858-526-4867. Fax: (877) 481-1781. E-mail: peipei.kung@pfizer.com.

■ ACKNOWLEDGMENT

We are grateful to Dr. Bob Almassy for solving the cocrystal structure of compound **6** bound to Hsp90, to Muhammad Alimuddin for analytical support, to the Pfizer La Jolla Analytical Group for compound purification, and to Drs. Henry Cheng and Martin Edwards for helpful discussions.

■ ABBREVIATIONS USED

Akt, serine-threonine kinase Akt; *t*-BuOH, *tert*-butyl alcohol; CDK4, cyclin-dependent kinase 4, serine−threonine kinase; DCM, dichloromethane; DIPEA, diisopropylethylamine; DMF, dimethylformamide; DMPK, drug metabolism and pharamcokinetics; DMSO, dimethylsulfoxide; EtOAc, ethyl acetate; Et_2O, diethyl ether; Her2, human epidermal growth factor receptor 2 protein; Hif1α, hypoxia-inducible factor 1α, a transcription factor; HTS, high throughput screening; LC−MS/MS, liquid chromatography−mass spectrometry; MeOH, methanol; PK/PD, pharmacokinetic/pharmacodynamic; *i*-PrOH, isopropanol; Raf, serine−threnonine kinase Raf; t_R, retention time; TEA, triethylamine; THF, tetrahydrofuran; TLC, thin layer chromatography

■ REFERENCES

(1) Lai, B.-T.; Chin, N. W.; Stanek, A. E.; Keh, W.; Lanks, K. W. Quantitation and intracellular localization of the 85K heat shock protein by using monoclonal and polyclonal antibodies. *Mol. Cell. Biol.* **1984**, *4*, 2802–2810.

(2) Workman, P.; Maloney, A. Hsp90 as a new therapeutic target for cancer therapy: the story unfolds. *Expert Opin. Biol. Ther.* **2002**, *2*, 3–24.

(3) (a) Xu, W.; Mimnaugh, E.; Rosser, M. F.; Nicchitta, C.; Marcu, M.; Yarden, Y.; Neckers, L. Sensitivity of mature ErbB2 to geldanamycin is conferred by its kinase domain and is mediated by the chaperone protein 90. *J. Biol. Chem.* **2001**, *276*, 3702–3708. (b) Sato, S.; Fujita, N.; Tsuruo, T. Modulation of AKT kinase activity by binding to Hsp90. *Proc. Natl. Acad. Sci. U.S.A.* **2000**, *97*, 10832–10837.

(4) Prodromou, C.; Siligardi, G.; O'Brien, R.; Woolfson, D. N.; Regan, L.; Panaretou, B. Regulation of Hsp90 ATPase activity by tetratricopeptide repeat (TPR)-domain co-chaperones. *EMBO J.* **1999**, *18*, 754–762.

(5) Dutta, R.; Inouye, M. GHKL, an emergent ATPase/kinase superfamily. *Trends Biochem. Sci.* **2000**, *25*, 24–28.

(6) Obermann, W. M. J.; Sondermann, H.; Russo, A. A.; Pavletich, N. P.; Hartl, F. U. In vivo function of Hsp90 is dependent on ATP binding and ATP hydrolysis. *J. Cell Biol.* **1998**, *143*, 901–910.

(7) Whitesell, L.; Mimnaugh, E. G.; De Costa, B.; Myers, C. E.; Neckers, L. M. Inhibition of heat shock protein HSP90-pp60v-src heteroprotein complex formation by benzoquinone ansamycins: essential role for stress proteins in oncogenic transformation. *Proc. Natl. Acad. Sci. U.S.A.* **1994**, *91*, 8324–8328.

(8) Guo, W.; Reigan, P.; Siegel, D.; Ross, D. Enzymatic reduction and glutathione conjugation of benzoquinone ansamycin heat shock protein 90 inhibitors: relevance for toxicity and mechanism of action. *Drug Metab. Dispos.* **2008**, *36*, 2050–2057.

(9) Solit, D. B.; Ivy, S. P.; Kopil, C.; Sikorski, R.; Morris, M. J.; Slovin, S. F.; Kelly, W. K.; DeLaCruz, A.; Curley, T.; Heller, G.; Larson, S.; Schwartz, L.; Egorin, M. J.; Rosen, N.; Scher, H. I. Phase 1 trial of 17-allylamino-17-demthoxygeldanamycin in patients with advance cancer. *Clin. Cancer Res.* **2007**, *13*, 1775–1782.

(10) Sydor, J. R.; Normant, E.; Pien, C. S.; Porter, J. R.; Ge, J.; Grenier, L.; Pak, R. H.; Ali, J. A.; Dembski, M. S.; Hudak, J.; Patterson, J.; Penders, C.; Pink, M.; Read, M. A.; Sang, J.; Woodward, C.; Zhang, Y.; Grayzel, D. S.; Wright, J.; Barrett, J. A.; Palombella, V. J.; Adams, J.; Tong, J. K. Development of 17-allylamino-17-dimethoxygeldanamycin hydroquinone hydrochloride (IPI-504), an anti-cancer agent directed against Hsp90. *Proc. Natl. Acad. Sci. U.S.A.* **2006**, *103*, 17408–17413.

(11) Janin, Y. L. ATPase inhibitiors of heat shock protein 90, second season. *Drug Discovery Today* **2010**, *15*, 342–353.

(12) Kasibhatla, S. R.; Hong, K.; Biamonte, M. A.; Busch, D. J.; Karjian, P. L.; Sensintaffar, J. L.; Kamal, A.; Lough, R. E.; Brekken, J.; Lundgren, K.; Grecko, R.; Timony, G. A.; Ran, Y.; Mansfield, R.; Fritz, L. C.; Ulm, E.; Burrows, F. J.; Boehm, M. F. Rationally designed high-affinity 2-amino-6-halopurine heat shock protein 90 inhibitors that exhibit potent antitumor activity. *J. Med. Chem.* **2007**, *50*, 2767–2778.

(13) Huang, K. H.; Veal, J. M.; Fadden, R. P.; Rice, J. W.; Eaves, J.; Strachan, J.-P.; Barabasz, A. F.; Foley, B. E.; Barta, T. E.; Ma, W.; Silinski, M. A.; Hu, M.; Partridge, J. M.; Scott, A.; DuBois, L. G.; Freed, T.; Steed, P. M.; Ommen, A, J.; Smith, E. D.; Hughes, P. F.; Woodward, A. R.; Hanson, G. J.; McCall, W. S.; Markworth, C. J.; Hinkley, L.; Jenks, M.; Geng, L.; Lewis, M.; Otto, J.; Pronk, B.; Verleysen, K.; Hall, S. E. Discovery of novel 2- aminobenzamide inhibitors of heat shock protein 90 as potent, selective, and orally active antitumor agents. *J. Med. Chem.* **2009**, *52*, 4288–4305.

(14) Brough, P. A.; Barril, X.; Borgognoni, J.; Chene, P.; Davies, N. G. M.; Davis, B.; Drysdale, M. J.; Dymock, B.; Eccles, S. A.; Garcia-Echeverria, C.; Fromont, C.; Hayes, A.; Hubbard, R. E.; Jordan, A. M.; Jensen, M. R.; Massey, A.; Merrett, A.; Padfield, A.; Parsons, R.; Radimerski, T.; Raynaud, F. I.; Robertson, A.; Roughley, S. D.; Schoepfer, J.; Simmonite, H.; Sharp, S. Y.; Surgenor, A.; Valenti, M.; Walls, S.; Webb, P.; Wood, M.; Workman, P.; Wright, L. Combining hit identification strategies: fragment-based and in silico approaches to orally active 2-aminothieno[2,3-*d*]pyrimidine inhibitors of the Hsp90 molecular chaperone. *J. Med. Chem.* **2009**, *52*, 4794–4809.

(15) Hopkins, L. A.; Groome, C. R.; Alex, A. Ligand efficiency: a useful metric for lead selection. *Drug Discovery Today* **2004**, *9*, 430–431.

(16) (a) Lesson, P. D.; Springthorpe, B. The influence of drug-like concepts on decision-making in medicinal chemistry. *Nat. Rev. Drug Discovery* **2007**, *6*, 881–890. (b) Ryckmans, T.; Edwards, M. P.; Horne, V. A.; Correia, A. M.; Owen, D. R.; Thompson, L. R.; Tran, I.; Tutt, M. F.; Young, T. Rapid assessment of a novel series of selective CB_2 agonists using parallel synthesis protocols: a lipophilic efficiency (LipE) analysis. *Bioorg. Med. Chem. Lett.* **2009**, *19*, 4406–4409.

(17) Sides, G. D.; Leschinger, M. I.; Walenta, R.; McNay, J. L., Jr. The tolerability and adverse event profile of moxonidine. *Rev. Contemp. Pharmacother.* **1998**, *9*, 491–499.

(18) Kung, P.-P.; Huang, B.; Zhang, G.; Zhou, J. Z.; Wang, J.; Digits, J. A.; Skaptason, J.; Yamazaki, S.; Neul, D.; Zientek, M.; Elleraas, J.; Mehta, P.; Yin, M.-J.; Hickey, M. J.; Gajiwala, K. S.; Rodgers, C.; Davies, J. F.; Gehring, M. R. Dihydroxyphenylisoindoline amides as orally bioavailable inhibitors of the heat shock protein 90 (Hsp90) molecular chaperone. *J. Med. Chem.* **2010**, *53*, 499–503.

(19) Mehta, P. P.; Kung, P.-P.; Yamazaki, S.; Walls, M.; Shen, A.; Nguyen, L.; Gehring, M.; Los, G.; Smeal, T.; Yin, M.-J. A novel class of specific Hsp90 small molecule inhibitors demonstrate in vitro and in vivo anti-tumor activity in human melanoma cells. *Cancer Lett.* **2011**, *300*, 30–39.

(20) Diaz, G. J.; Daniell, K.; Leitza, S. T.; Martin, R. L.; Su, Z.; McDermott, J. S.; Cox, B. F.; Gintant, G. A. The [^{3}H]dofetilide binding assay is a predictive screening tool for hERG blockade and proarrhythmia: comparison of intact cell and membrane preparations and effects of altering $[K^+]_o$. *J. Pharmacol. Toxicol. Methods* **2004**, *50*, 187–199.

(21) Kreusch, A.; Han, S.; Brinker, A.; Zhou, V.; Choi, H.-S.; He, Y.; Lesley, S. A.; Caldwell, J.; Gu, X.-J. Crystal structures of human Hsp90a-complexed with dihydroxyphenylprazoles. *Bioorg. Med. Chem. Lett.* **2005**, *15*, 1475–1478.

(22) van Breeman, R. B.; Li, Y. Caco-2 cell permeability assays to measure drug absorption. *Expert Opin. Drug Metab. Toxicol.* **2005**, *1*, 175–185.

(23) Tseng, G. N. Ikr The hERG channel. *J. Mol. Cell. Cardiol.* **2001**, *33*, 835–849.

(24) Giuliano, C.; Jairaj, M.; Zafiu, C. M.; Laufer, R. Direct determination of unbound intrinsic drug clearance in the microsomal stability assay. *Drug Metab. Dispos.* **2005**, *33*, 1319–1324.

(25) Brough, P. A.; Aherne, W.; Barril, X.; Borgognoni, J.; Boxall, K.; Cansfield, J. E.; Cheung, K.-M. J.; Collins, I.; Davies, N. G. M.; Drysdale, M.; Dymock, B.; Eccles, S. A.; Finch, H.; Fink, A.; Hayes, A.; Howes, R.; Hubbard, R. E.; James, K.; Jordan, A. M.; Lockie, A.; Martins, V.; Massey, A.; Matthews, T. P.; McDonald, E.; Northfield, C. J.; Pearl, L. H.; Prodromou, C.; Ray, S.; Raynaud, F. I.; Roughley, S. D.; Sharp, S. Y.; Surgenor, A.; Walmsley, D. L.; Webb, P.; Wood, M.; Workman, P.; Wright, L. 4,5-Diarylisoxazole Hsp90 chaperone inhibitors: potential therapeutic agents for the treatment of cancer. *J. Med. Chem.* **2008**, *51*, 196–218.

(26) Chessari, G.; Congreve, M. S.; Callaghan, O.; Cowan, S. R.; Murray, C. W.; Woolford, A. J.-A.; O'Brien, M. A.; Woodhead, A. J. PCT Int. Appl. 2006123165, 2006.

(27) Hossain, M. T.; Timberlake, J. W. Synthesis of bisbicyclo-[1.1.1]pentyldiazene. The smallest bridgehead diazene. *J. Org. Chem.* **2001**, *66*, 6282–6285.

(28) Dow, R. L.; Carpino, P. A.; Hadcock, J. R.; Black, S. C.; Iredale, P. A.; DaSilva-Jardine, P.; Schneider, S. R.; Paight, E. S.; Griffith, D. A.; Scott, D. O.; O'Connor, R. E.; Nduaka, C. I. Discovery of 2-(2-chlorophenyl)-3-(4-chlorophenyl)-7-(2,2-difluoropropyl)-6,7-dihydro-2*H*-pyrazolo[3,4-*f*][1,4]oxazepin-8-(5*H*)-one (PF-514273), a novel, bicyclic lactam-based cannabinoid-1 receptor antagonist for the treatment of obesity. *J. Med. Chem.* **2009**, *52*, 2652–2655.

(29) McHugh, M.; Proctor, G. R. Ring expansion of some heterocyclic β-keto esters with dimethyl acetylenedicarboxylate. Part 2. Synthesis of azepine, azocine, benzazocine, and benzazonine derivatives. *J. Chem. Res., Miniprint* **1984**, 2230–2253.

(30) Lau, J. F.; Jeppesen, C. B.; Rimvall, K.; Hohlweg, R. Ureas with histamine H3-antagonist receptor activity—a new scaffold discovered by lead-hopping from cinnamic acid amides. *Bioorg. Med. Chem. Lett.* **2006**, *16*, 5303–5308.

(31) Blaszykowski, C.; Aktoudianakis, E.; Bressy, C.; Alberico, D.; Lautens, M. Preparation of annulated nitrogen-containing heterocycles via a one-pot palladium-catalyzed alkylation/direct arylation sequence. *Org. Lett.* **2006**, *8*, 2043–2045.

(32) England, K.; Mason, H.; Osborne, R.; Roberts, L. An improved synthesis of a novel α_{1A} partial agonist including a new two-step synthesis of 4-fluoropyrazole. *Tetrahedron Lett.* **2010**, *51*, 2849–2851.